

DSpace Institution

DSpace Repository

<http://dspace.org>

Communication System Engineering

thesis

2022-08

Performance Analysis of Downlink Massive MIMO System with Precoding Techniques and Pilot Reuse Factor

Gebey, Admassu

<http://ir.bdu.edu.et/handle/123456789/14460>

Downloaded from DSpace Repository, DSpace Institution's institutional repository



BAHIR DAR UNIVERSITY

BAHIR DAR INSTITUTE OF TECHNOLOGY

SCHOOL OF GRADUATE STUDIES

FACULTY OF ELECTRICAL AND COMPUTER ENGINEERING

Performance Analysis of Downlink Massive MIMO System with Precoding Techniques and Pilot Reuse Factor

By

GEBEY ADMASSU

A Thesis Submitted to the School of Graduate Studies of Bahir Dar Institute
of Technology in Partial Fulfillment of the Requirements for the Degree of

Master of Science
in Communication System Engineering

August 2022

Bahir Dar, Ethiopia

Bahir Dar University

Bahir Dar Institute of Technology

School of Graduate Studies

Faculty of Electrical and Computer Engineering

**Performance Analysis of Downlink
Massive MIMO System with
Precoding Techniques and Pilot
Reuse Factor**

By

Gebey Admassu

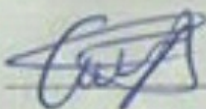
Adviser:

Dr. Fikreselam Gared (Associate Professor)

Declaration

I declare that this thesis titled, 'Performance Analysis of Downlink Massive MIMO System with Precoding Techniques and Pilot Reuse Factor' is my own original work. All sources of materials used for the thesis has been clearly stated and attributed.

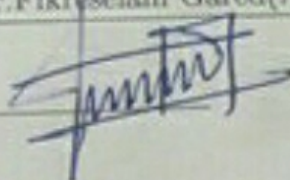
Student Name: Gebey Admassu

Signature: 

Date of submission: Aug/12/2022

This thesis has been submitted for examination with my approval as a university adviser.

Advisor Name: Dr. Fikreselam Gared (Asso. professor)

Advisor's Signature: 

Date: Aug/12/2022

BAHIR DAR UNIVERSITY

BAHIR DAR INSTITUTE OF TECHNOLOGY

SCHOOL OF RESEARCH AND POSTGRADUATE STUDIES

FACULTY OF ELECTRICAL AND COMPUTER ENGINEERING

Approval of thesis for defense result

I hereby confirm that the changes required by the examiners have been carried out and incorporate in the final thesis.

Name of Student: Gebey Admassu Signature: [Signature] Date: 13 Aug 2022

As members of the board examiners, we examined this thesis entitled 'Performance Analysis of Downlink Massive MIMO System with Precoding Techniques and Pilot Reuse Factor'. We hereby certify that this thesis is accepted for fulfilling of the requirements for the award of the Degree of Master of Science in Communication System Engineering.

Board of Examiners

Name of Advisor

Dr. Fikreselam Gared

Signature

[Signature]

Date

12/Aug 2022

Name of External Examiner

Dr. Yibnew Wondie

Signature

[Signature]

Date

10-August-2022

Name of Internal Examiner

Dr. Amare Kereaw

Signature

[Signature]

Date

18 Aug. 2022

Name of Chairperson

Mr. Tadie Birhan

Signature

[Signature]

Date

13 Aug 2022

Name of Chair Holder

Mr. Tadie Birhan

Signature

[Signature]

Date

13 Aug 2022

Name of Faculty Dean

Tewodros C

Signature

[Signature]

Date

17/12/2019



Faculty Stamp

Abstract

Massive MIMO (Ma-MIMO) is one of the basic enabler technologies for 5G wireless communication networks to provide higher spectral efficiency (SE) by using large number of antennas and serves many users simultaneously in the same frequency–time resources. In a Ma-MIMO downlink (DL) system, the base station (BS) estimates the channel using uplink (UL) training but a pilot contamination (PC) is the major challenge in multi-cell Ma-MIMO system. This challenge causes severe inter-cell Interference at the home cell and then limits the performance of the system. Precoding techniques with pilot reuse factor (PRF) are used to mitigate the PC effect. The performance of DL multicell Ma-MIMO system is analyzed under spatial correlated Rayleigh fading channel with both perfect and imperfect channel state information (CSI). Precoding is used to mitigate the intra-cell interferences and PRF reduces the PC effect by assigning orthogonal pilots to neighboring cells. SE performance of multi cell Ma-MIMO system is analyzed with maximum ratio transmitter (MRT), zero forcing (ZF) and minimum mean square error (MMSE) precoding techniques and combined with PRF. Performance comparison of precoding techniques showed that MMSE provides the best SE performance for both CSI and it has highest SE at PRF of four among all when the number of antennas are changed. When both the number of users and antennas are increased simultaneously and $M \gg K$, the SE is improved by more than 25% and also system performance with perfect CSI is better than imperfect CSI.

Key Words: CSI, Ma-MIMO, PRF, PC, Precoding

Acknowledgment

First and Foremost, I would like to express thanks to almighty of God for giving strength and blessing me to complete the thesis successfully.

I would like to thank to my thesis Advisor, Dr. Fikreselam Gared with my deepest and heartfelt gratitude for his help during the selection of thesis title, constant encouragement, expert academic and guidance throughout this thesis work. I have got many things from him. He has taught me not only academic knowledge but also critical thinking, commitment and inspiration for every aspect. I thank him specially for providing knowledge about Latex and the way how to describe the methodology of research.

I also would like to thank all the postgraduate instructors of communication systems Engineering in field of ECE for providing best education and developing my insight to research. Finally, I am thankful to my family for their love and friends for helping me until the end of this thesis work.

Contents

Declaration	ii
Abstract	iv
Acknowledgment	v
List of Figures	viii
List of Tables	x
Abbreviations	xi
Symbols	xiii
1 Introduction	1
1.1 Background	1
1.2 Multicell Ma- MIMO System and Pilot Contamination	6
1.3 Statement of the Problem	6
1.4 Objective	7
1.4.1 General Objective	7
1.4.2 Specific objectives	7
1.5 Research Methodology	8
1.6 Thesis Contribution	9
1.7 Scope Of The Thesis	10
1.8 Thesis Organization	11
2 Literature Review	12
3 System and Channel Model of DL Ma-MIMO Systems	17
3.1 System Model	17
3.2 Propagation Channel Model	19
3.3 Local Scattering based Spatial Channel Correlation Model	21
3.4 Channel Estimation	23

3.4.1	Uplink Training Phase (Uplink Pilot Transmission) Based Channel Estimation	24
3.4.2	MMSE based Channel Estimation	26
3.5	Pilot Contamination	26
3.6	Perfect and Imperfect CSIT	28
3.6.1	Perfect CSIT	28
3.6.2	Imperfect CSIT	28
3.7	Pilot Reuse Factor	28
3.8	Signal Model of Downlink Data Transmission	31
3.8.1	DL Data Transmission	31
3.9	Precoding Techniques	32
3.10	Spectral Efficiency with Perfect and Imperfect CSI	34
3.10.1	Spectral Efficiency with Perfect CSI	34
3.10.2	Spectral Efficiency with Imperfect CSI	37
4	Simulation Results and Discussion	42
4.1	Simulation setup	42
4.2	Spectral Efficiency for different number of BS antennas with imperfect CSI	45
4.3	Spectral Efficiency versus different number of users with imperfect CSI .	48
4.4	Spectral Efficiency for different number of users and number of antennas with imperfect CSI	50
4.5	Spectral Efficiency for different number of BS antennas with perfect CSI	52
4.6	Spectral Efficiency for both different number of users and BS antennas with perfect CSI	53
5	Conclusion and Future Works	56
5.1	Conclusion	56
5.2	Recommendations for Future Work	57
	Bibliography	58

List of Figures

Figure 1.1	A SU-MIMO system [6]	2
Figure 1.2	Downlink Multiuser MIMO System [8]	3
Figure 1.3	Downlink Massive MIMO System [14]	4
Figure 1.4	Block diagram that describes flow of work	8
Figure 1.5	Block diagram of system work methodology	10
Figure 3.1	Three Cells Multi-user Downlink TDD-Massive MIMO System Model	18
Figure 3.2	NLOS propagation under local scattering spatial correlation model [29]	21
Figure 3.3	Time-division duplex Protocol [3]	24
Figure 3.4	Uplink Pilot Contamination in a multi cell scenario where BS i in cell i receive pilots from adjacent cell [23]	27
Figure 3.5	Cellular hexagonal cell with $N=3$ [3]	29
Figure 3.6	Cellular hexagonal cell with $N=4$ [3]	30
Figure 3.7	Block diagram of the linear precoder at each BS [3]	31
Figure 3.8	: Block diagram representation of a multi-cell DL Ma-MIMO sys- tem with linear precoding [3]	32
Figure 4.1	16-cell cluster with pilot reuse $N= 4$	43
Figure 4.2	12-cell cluster with pilot reuse $N= 3$	44
Figure 4.3	16-cell cluster with pilot reuse $N= 1$	44
Figure 4.4	Average sum SE with respect to the number of BS antennas for M-MMSE, ZF and MRT precoding techniques (for a PRF of one and $K=10$)	45
Figure 4.5	Average sum SE with respect to the number of BS antennas for M-MMSE, ZF and MRT precoding techniques (for a PRF of three and $K=10$)	46
Figure 4.6	Average sum SE with respect to the number of BS antennas for MMSE, ZF and MRT precoding techniques a PRF of four and $K=10$	47

Figure 4.7	Average sum SE with respect to the number of users for M-MMSE, ZF and MRT precoding techniques (a PRF of one and M=100) . . .	48
Figure 4.8	Average sum SE with respect to the number of users for M-MMSE, ZF and MRT. Precoding techniques (for a PRF of three and M=100) . . .	49
Figure 4.9	Average sum SE with respect to the number of users for MMSE, ZF and MRT precoding techniques and a PRF of four (M=100) . . .	50
Figure 4.10	Average sum SE with respect to the number of antennas for M-MMSE, ZF and MRT precoding techniques (for a PRF=4 and K=10)	51
Figure 4.11	Average sum SE with respect to the number of antennas for MMSE, ZF and MRT precoding techniques(for a PRF=4 and K=20) . . .	52
Figure 4.12	Average sum SE with respect to the number of BS antennas for MMSE, ZF and MRT precoding techniques (for K=10 and SNR=5dB) . . .	53
Figure 4.13	Average sum SE with respect to the number of antennas for MMSE, ZF and MRT precoding techniques (for K=10 and SNR=0dB) . . .	54
Figure 4.14	Average sum SE with respect to the number of antennas for MMSE, ZF and MRT precoding techniques(for K=20 and SNR=0dB) . . .	55

List of Tables

Table 4.1	parameters and values	43
Table 4.2	SE values at specified values of BS antennas in the range $M=10$ to 110 and number of users per cell ($K=10$)	50
Table 4.3	SE numerical values at specified values of BS antennas in the range $M=10$ to 110 and number of users per cell ($K=20$)	51
Table 4.4	SE numerical values at specified values of BS antennas in the range $M=10$ to 110 and number of users per cell ($K=10$)	54
Table 4.5	SE numerical values at specified values of BS antennas in the range $M=10$ to 110 and number of users per cell ($K=20$)	55

Abbreviations

ASD	A ngular S tandard D eviation
AWGN	A dditive W hite G aussian N oise
BS	B ase S tation
CSI	C hannel S tate I nformation
CSIT	C hannel S tate I nformation at T ransmitter
DL	D own L ink
DPC	D irty P aper C oding
EE	E nergy E fficiency
FDD	F requency D ivision D uplexing
I.I.D	I ndependent and I dentical D istribution
LTE	L ong T erm E volution
Ma-MIMO	M assive M ultiple I nput M ultiple O utput
MATLAB	M atrix L abratory
MIMO	M ultiple I nput M ultiple O utput
MIMO	M inimum M ean S quare E rror
M-MMSE	M ulticell M inimum M ean S quare E rror
MRC	M aximum R atio C ombinning
MRT	M aximum R atio T ransmission
MU-MIMO	M ulti U ser M ultiple I nput M ultiple O utput
NLOS	N on L ine O f S ight
PC	P ilot C ontamination
PRF	P ilot R euse F actor
RZF	R egularized Z ero F orcing
SDMA	S pace D ivissio M ultiple A ccess
SE	S pectral E fficiency
SINR	S ignal I nterference N oise R atio
SNR	S ignal N oise R atio
SU-MIMO	S ngle U ser M ultiple I nput M ultiple O utput
TDD	T ime D ivision D uplexing
THP	T omlinson H arashima P recoding

UE	User Equipment
ULA	Uniform Linear Array
UL	Up Link
ZF	Zero Forcing

Symbols

$ \cdot $	Absolute value (cardinality of a set)
B_c	Coherence bandwidth
C	An element of complex values
σ	Noise variance
N_C	Complex Normal distribution
α	Pathloss exponent
β	Large scale coefficient
φ	Nominal angle
σ_φ	Angular standard deviation
σ_{sh}	Standard deviation of the shadow fading
τ_c	Coherence block
τ_d	Downlink data
τ_p	Uplink Pilot
τ_u	Uplink data
d	Distance between the transmitter and the receiver
Υ	Median channel gain
φ_n	Arrival angle
F	Log-normal shadowing
N	Normal distribution
$tr(\cdot)$	Trace operator
$(\cdot)^{-1}$	Inverse operator
$(\cdot)^T$	Transpose operator
$(\cdot)^H$	Hermitian operator
i	Cell i index
k	User index
j	Cell j index
l	Cell l index
m	Antenna index
K	Number of Scheduled users
M	Number of total antennas at BS

L	Number of total cells
R	Spatial channel correlation
T_c	Coherence time

Introduction

1.1 Background

The needs for capacity in wireless communications have been increasing continuously. But the effect of multipath fading, limited power at the transmitter and scarce spectrum (the available radio spectrum is limited) are challenging extremely for the designing of high SE, high reliability wireless communication systems and the capacity of the system needs cannot be achieved without a significant increase in SE. MIMO technology is used to mitigate this challenge [1]. MIMO is a technology that uses multiple antennas at both transmission and reception. When the number of antennas at the transmitter and receiver increases, the degree of freedom in propagation channel increases and gives an improvement in SE and the data rate or link reliability [1][2]. Additionally, the efficiency of a wireless network may be improved by deploying access points more densely, using more spectrum and increasing the SE [3]. Since the radio-frequency spectrum is scarce resource, researches over the last years have been focused towards improving SE so that higher SE can be achieved within a given bandwidth using the MIMO and Ma-MIMO technology that are used adaptively according to channel condition between source and destination. MIMO technology can be logically classified into one of three categories: point-to-point MIMO, Multi user -MIMO (MU-MIMO), and Ma-MIMO [4].

(i) Point-to-Point MIMO (Single User(SU)-MIMO)

A MIMO technique were first investigated in point-to-point MIMO (SU-MIMO). It uses multiple antennas at the transmitter communicated with multiple antennas at the receiver and serves a single user. SU-MIMO gives higher SE, data transmission rate and transmission reliability than Single Input Single Output (SISO) wireless systems. Some of the technologies that depend on MIMO systems are IEEE 802.11, third Generation (3G) and Long Term Evolution (LTE) where the LTE standard uses up to eight antennas on both BS and terminals side [4][5]. As shown in Figure 1.1 M and N number of

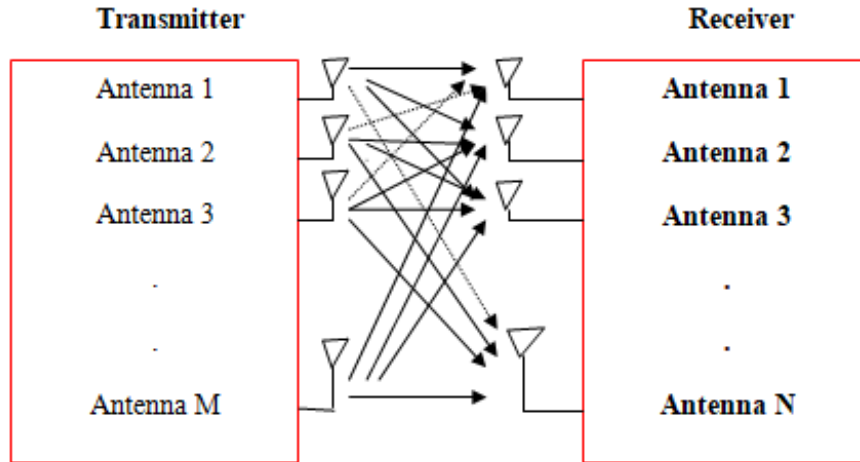


Figure 1.1: A SU-MIMO system [6]

antennas at the transmitter and receiver are described in SU-MIMO system, respectively. In this system, a single transmitter transmits information to a single receiver. The data intended for the receiver are processed and transformed into the transmit signals to be sent from M BS antennas [6]. But in point-to-point MIMO, energy power consumption of the signal processing units and the hardware complexity increase at both sides [2]. It has unfavorable propagation and is not scalable. The unfavorable propagation can be minimized using MU-MIMO in which the multiple antenna at the receiver side is divided into many independent terminal users.

(ii) MU-MIMO

The MU-MIMO is upgraded from the point-to-point MIMO by breaking up the K -antenna terminal into multiple autonomous terminals. In MU-MIMO system, the BS communicates with MU terminals simultaneously using the same time-frequency resources. Multiple antenna is implemented in both UL and DL communication. In the UL a group of users transmits to the same BS whereas in DL a BS broadcast data streams to MUs at the same frequency and time. MU-MIMO are designed to work both in Time Division Duplex (TDD) and Frequency Division Duplex (FDD) mode [7].

It uses dirty-paper coding (DPC) or receiver detector to mitigate the interference. DPC is a nonlinear precoding technique. It is a multi-user precoding strategy based on interference pre-subtraction and it is also an optimal strategy. It is difficult to implement in

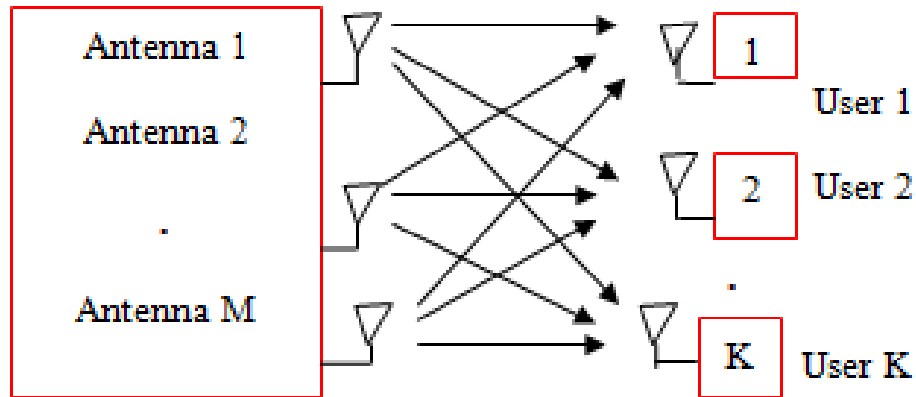


Figure 1.2: Downlink Multiuser MIMO System [8]

practical systems especially when the numbers of users increase due to its high computational complexity [9]. To minimize the computational complexity of DPC a sub-optimal linear pre-processing techniques commonly known as precoding or beam forming is applied on the transmitted signal. Precoding strategies include a channel inversion variants and a simple conjugate of a channel are common in MU-MIMO system. The knowledge of CSI at the transmitter is required to handle the interferences. In the DL, in the absence of channel state information at the transmitter (CSIT), user multiplexing is generally not possible, as the BS just does not know in which direction to form spatial beams [10][11]. On the DL both the BS and the terminals have to know the CSI, which requires substantial resources to be set aside for transmission of pilots in both directions, and which causes complexity as the number of antennas increased [12]. Due to these challenges, conventional MU-MIMO is not scalable with respect to the number of BS antennas and scheduled users [3][13].

(iii) Ma-MIMO Systems

Ma - MIMO is a MU-MIMO system where a BS with a large number of antennas array serve MU terminals simultaneously, each having a single antenna or more antennas, in the same time-frequency resource [2]. It has been proposed as a solution to scalability and uses simple linear signal processing both on the UL and DL. In Ma- MIMO (M antennas is much larger than K users), only the BS requires and learns channel and operates in TDD mode to exploit channel reciprocity. Sending UL pilots and exploiting channel reciprocity are used for CSI acquisition. In Ma-MIMO systems, deploying large number of

antennas at the BS focuses the transmit energy into smaller regions. This leads high improvement in radiated SE and energy efficiency (EE). The SE improvement results from spatial multiplexing gains and the improvement in EE is obtained due to concentration of energy in small regions [2][13]. Thus, Ma-MIMO is expected to increase the radiated

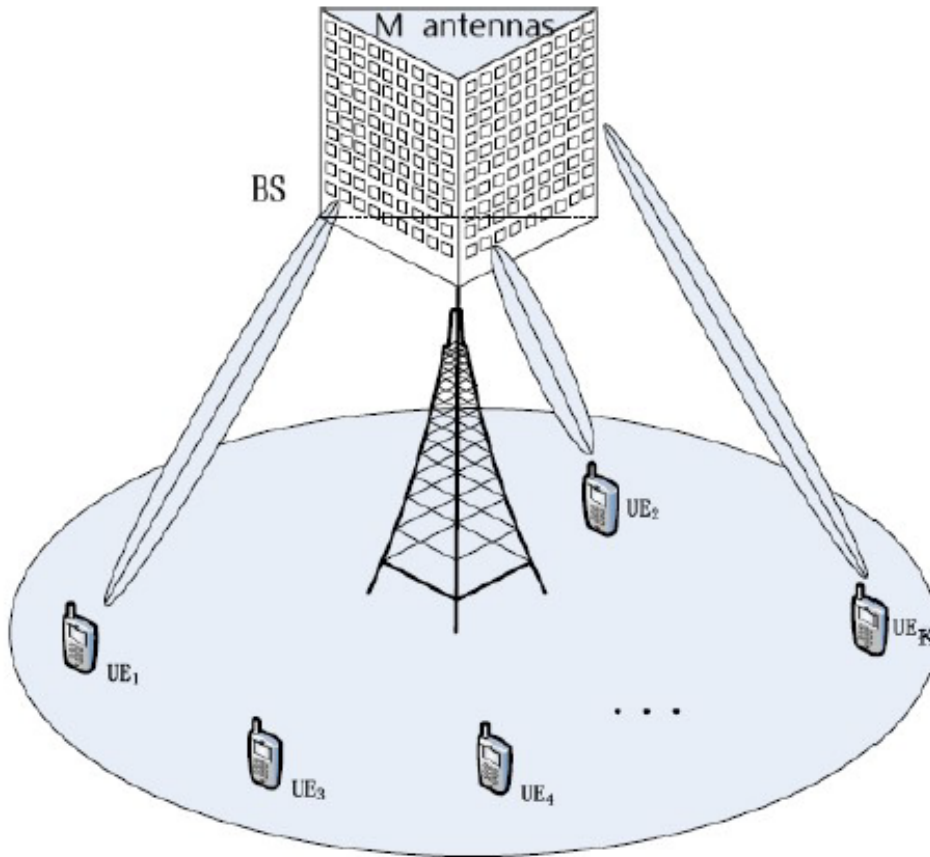


Figure 1.3: Downlink Massive MIMO System [14]

EE in the order of $100\times$ and the SE in the order of $10\times$ [2][12][15]. Ma-MIMO is one of the key technology for the next generation of wireless communication networks (5G) due to its higher SE, EE, enhance link reliability, boost the channel capacity, and connection density. The block diagram of DL Ma-MIMO system with M antennas and K users is shown in Figure 1.3.

Generally, the main benefits of Ma-MIMO systems are described as follows:

- **High SE and reliability of communication** : for M -antennas at the BS and K -users in Ma- MIMO systems can achieve a diversity order of M and multiplexing gain of K [2][12]. As a result, we can gain high reliability of communication and high SE by increasing both M and K [2][3].

- **High EE:** the gain in EE enables Ma- MIMO systems to operate with low radiated power as compared to other mobile networks. This helps to minimize the energy consumption by cellular systems and to save energy. Additionally, networks that consume low power could be powered by green energy sources such as wind energy and solar energy [16]. Thus, they can be deployed where no electricity grid is available. Besides, it is shown in [17] that the users uplink transmit power can be scaled down proportional to the number of antennas at the BS. This helps to elongate the battery life of user terminals.
- **Simplify signal processing complexity:** the use of large number of antennas at the BS helps to obtain favorable propagation condition where the channel vectors between the users and the BS become pair wisely orthogonal. Under favorable propagation¹ [18], the effect of inter user interference and noise can be eliminated with simple signal processing techniques. Hence, linear processing techniques such as liner precoding in the DL and linear detection in the UL can be employed to get near optimal performance [3][12].
- **Channel hardening in large dimension:** the effect of small scale fading is averaged out and the channel becomes nearly deterministic when the numbers of antennas at the BS are very large. That is, when the channel matrix is large, the distribution of the eigenvalues becomes less sensitive to the actual distribution of the channel and this property is termed as channel hardening [19]. Channel hardening allows simple linear detection and precoding algorithms to achieve near optimal performance in large dimensions. Thus, user scheduling, power control, optimization and resource allocation can be done in large-scale fading instead of the small-scale fading. This simplifies the signal processing complexity [17].

Although Ma-MIMO systems provide many gains to the current capacity demand, It has also many technical challenges like channel state acquisition and channel modeling, complexity of inverse operation in linear processing, MU interference and user scheduling, resource allocation algorithms and complex power control, multicell operation and PC and complexities on deployment scenarios [3][20].

1.2 Multicell Ma- MIMO System and Pilot Contamination

Practical Ma-MIMO systems contain many cells even though PC is the major challenges in multi-cell Ma-MIMO systems. In a multi-cell scenario, user within each cell receives inter-cell interference in addition to intra-cell interference. The CSI of Ma-MIMO is estimated at the BS via UL training based on TDD. MUs send orthogonal signals which are known at the BS in the UL training. However, in TDD operation the coherence block is limited and unique orthogonal signals for all users in all cells cannot be realized. This indicates that orthogonal signals can be reused within a cell or in adjacent cells. This result intercell interference and channel estimation error. This effect is called PC. The intercell interference is because of pilot contamination and this restricts the system capacity [21]. Therefore, PC degrades the system performance and becomes one of the main reasons for the performance loss in Ma-MIMO systems.

To alleviate this problem and analyze the performance of multi-cell Ma-MIMO systems various researches have been conducted using different schemes or techniques like precoding, channel estimation and pilot scheduling.

In this thesis work the performance of DL multi-cell Ma-MIMO system is analyzed using PRF and linear precoding techniques. We used low complexity precodings techniques such as MRT, ZF and multi-cell minimum mean square error (M-MMSE) to minimize intracell interference by directing the signal to the intended user and nulls to unintended users and PRF one, three and four to reduce the inter-cell interference. M-MMSE is used to reduce intercell interference in addition to intracell interference.

1.3 Statement of the Problem

The Ma-MIMO system terminals use the same orthogonal pilots while UL training to estimate the channel at the BS. Due to the number of orthogonal pilot signals in a coherence block is limited, the orthogonal pilot sequences cannot be allocated for all

users among the cells, which results the reuse of the orthogonal pilots in adjacent cells. As a result, the same set of orthogonal pilots used in neighboring cells interfere with each other, and the obtained estimated channel at the BS in a given cell can be contaminated by pilots transmitted by users in other cells. This effect is known as pilot contamination and it is a challenge that reduces the performance of the system. To address this challenge PRF in combination with precoding techniques are used for multi cell Ma-MIMO DL TDD systems for both perfect and imperfect CSI. The system performance with both CSI and their comparison using precoding techniques and PRF in terms of SE is analyzed. PRF is used to reduce intercell interference and precoding techniques like MRT, ZF, and MMSE suppresses the intracell interferences.

1.4 Objective

1.4.1 General Objective

The general objective of this thesis is to analyze the performance of DL multi cell Ma-MIMO systems using linear precoding techniques and PRF.

1.4.2 Specific objectives

The specific objectives of our work includes:

- to review the precoding techniques in multi cell Ma-MIMO System.
- to investigate and analyze the effect of PC in multi cell ma-MIMO system.
- to analyze the system performance of DL multi cell Ma-MIMO systems with perfect and imperfect CSI.
- to derive SINR, SE and evaluate the SE using MRT, ZF and MMSE Precodings.
- to evaluate the SE using MRT, ZF and MMSE Precodings and one, three and four PRF for various number of antennas and users.

- to compare the performance of precoding techniques with PRF.

1.5 Research Methodology

In this study we follow procedural steps and methods in order to realize this thesis. The methods that should be followed to accomplish this thesis begin with reviewing the related works (different literature), read and collect data from books, and other related documents, modeling the system based on the inputs retrieved from review of related works and the statement of the problem in mind. Then simulate target network to evaluate the performance as per system model, mathematical description. Finally interpreting the result, discussion and conclusion will be prepared as shown in Figure 1.4.

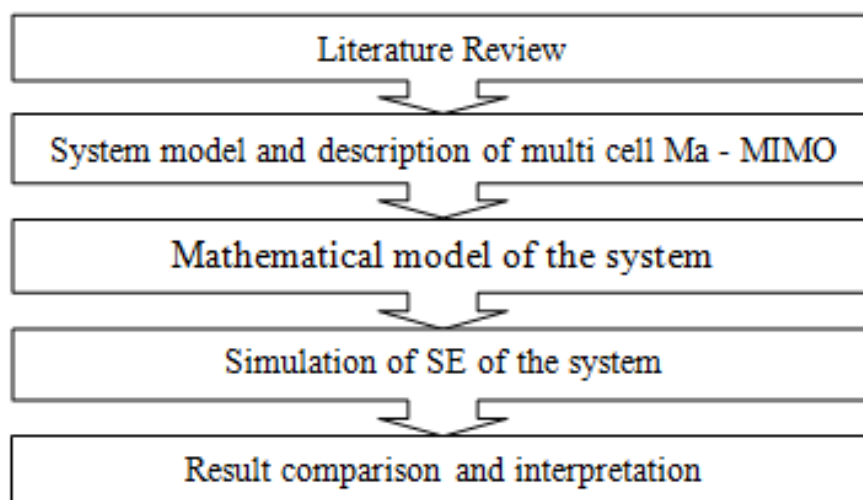


Figure 1.4: Block diagram that describes flow of work

- Determining the channel model and signal model (considering DL Multi cell Ma-MIMO TDD Systems and spatially correlated fading channel)
- Defining precoding techniques
- Calculating the SINR and SE of the system using precoding techniques for both perfect and imperfect CSI

- Identifying the parameters for a given simulation scenario
- Simulate target network to analyze the SE as the capacity of the system
- SE that results from using different precoding techniques, and combined them with PRF is evaluated and performance comparison is done.

The system uses both PRF and precodings to mitigate the PC and analyze its performance. The detail methodology diagram is shown in Figure 1.5. First estimate the channel responses of Ma-MIMO system at the BS using TDD mode via UL pilots and MMSE channel estimation. Then PRF greater than one is used to reduce PC (which is occur due to the use of the same pilot by user terminals in adjacent cell as home cell while sending UL). The PC is reduced by assigning orthogonal pilots to neighboring cells and next neighboring cells according to pilot group. According to the reuse pattern, a pilot group is assigned to each cell and the pilots are randomly distributed to the user terminals within that group as in the case of full pilot reuse. Precoding techniques are used to focus each signal at its desired user terminal and mitigate interference towards other terminals. Finally, the system performance is analyzed under both perfect and imperfect CST in terms of SE as capacity based on the used or selected precoding techniques and different PRF for different number of antennas and users.

1.6 Thesis Contribution

The contribution of the thesis work can be expressed as follows:

- A multi cell Ma-MIMO system with MRT, ZF and MMSE precoding techniques and PRF are presented. The system SE expressions of users under spatially correlated rayleigh fading channels are derived.
- Particularly, local scattering based spatial correlation channel model is considered to develop the NLOS multipath components between BS and users. (i.e. To formulate a correlated based channel model for multicell Ma - MIMO).

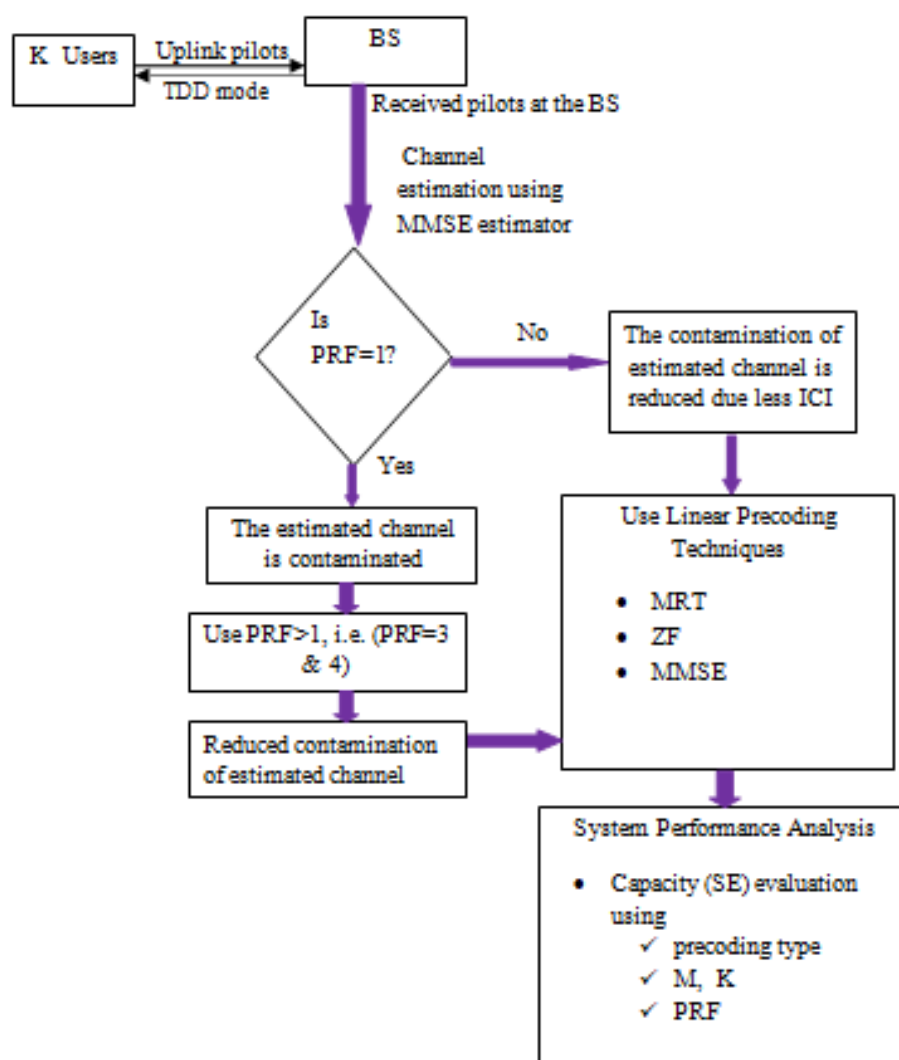


Figure 1.5: Block diagram of system work methodology

- Analysis and compare system performance of DL multi cell Ma-MIMO with MRT, ZF and MMSE precoding techniques and PRF in case of both perfect and imperfect CSI.

1.7 Scope Of The Thesis

The thesis focuses on the performance analysis of DL Ma-MIMO system using MRT, ZF and MMSE precodings with PRF based on key performance indicator which is limited to multi-cell DL scenario. The system depend on the availability of both perfect and

imperfect CSI at the BS with the assumption of spatially correlated Rayleigh fading channel model. Performance evaluations are done using software simulations.

1.8 Thesis Organization

The rest of the document is organized as follows

- **Chapter 2:** After describing about MIMO, MU-MIMO, Ma-MIMO, and their benefits and the challenges they faced, we present the background and recent works related to precoding techniques and PRF which aimed to solve the short coming of multi cell Ma-MIMO system.
- **Chapter 3 :**The system, channel and signal model is presented. Additionally, the SE with both perfect and imperfect CSI and the linear precoding techniques matrices are described both mathematically and theoretically.
- **Chapter 4 :** First we describe the simulation setup which describes how numerical simulation is performed. Then simulation results which depicts the average sum SE of multi cell DL Ma-MIMO system with different PRF and precoding techniques are presented. then discussions and interpretation are made based on each output of SE evaluations.
- **Chapter 5:** This chapter includes the conclusion of this thesis and recommendations which leads future work and further investigation on this work.

Literature Review

There are different types of research methods investigated the performance of the precoding and pilot assignment techniques to mitigate the issue associated with PC in multi cell Ma-MIMO system. Among these methods, the most related works are described as follow:

In [22] Xudong Zhu and Zhaocheng Wang proposed smart pilot assignment (SPA) method for Ma-MIMO to improve the users performance with severe PC. Authors motivated to maximize UL signal to interference noise ratio (SINR) by avoiding the pilot sequence with great inter-cell interference. Here, the pilots are assigned to the user having bad channel quality. The training sequence is assigned with the lowest inter-cell interference to the user having the worst channel quality in a sequential way according to the proposed schemes and by exploiting the large-scale characteristics of fading channels. They concerned on adjusting the combination between the users and pilot sequences and analyzed the system performance in terms of the minimum UL SINR with the average UL capacity of the user among in the target cell with respect to the number of antennas and in each cell convergence of the UL SINR; the average UL capacity of the user with the minimum UL SINR of SPA exceeds the conventional schemes by 0.6 bps/Hz. The system performance of the proposed scheme approaches to that of the optimal solution when large number of antennas is used. Finally, they concluded that the proposed SPA scheme provides better performance than random pilot assignment. But they did not consider inter-cell interference that causes the PC.

In [23] Zhao et al. suggested a combination of pilot contamination precoding (PCP) and pilot assignment to combat PC in multi-cell MU- Ma-MIMO systems. Authors used two heuristic pilot assignment schemes, such as a swapping-based and a greedy scheme combine with ZF-PCP and studied the system performance of the DL transmission in Ma-MIMO in terms of sum rate metrics as the number of BS antennas is increased and also studied the computational complexity of the proposed schemes by calculating the

number of search times. They formulated an optimization problem to find the best pilot assignment solution in PCP assisted Ma-MIMO systems which is used to maximize the sum rate of the system. They stated that the swapping-based scheme can achieve an increase of 16 percent in the sum rate, and the greedy scheme can achieve an increase of 13 percent when the number of antennas at BSs, M is large as 1000,

By analyzing the results, They conclude that the proposed methods perform better than the an existing PCP scheme with random pilot assignment and ZF-PCP scheme. These schemes provide improved system performance. But the PCP matrix is depend on the pilot assignment information and altered depending on the update in pilot assignment information.

In [22] and [24] a joint pilot, time-shifted and SPA assignment scheme has been proposed. Authors used time-shifted and the SPA schemes to mitigate PC effect. Time-shifted strategy is used to suppress Inter-group interference and intra-group is reduced by SPA scheme. According to their obtained simulation result the proposed scheme improved the performance of the system and provide better than the conventional pilot assignment schemes but the mutual interference between UL pilot signals and data cannot be eliminated even though the use of SPA scheme.

Ahmed S. Al-hubaishi in [24], proposed an efficient pilot assignment (EPA) scheme against PC in Multi cell Ma-MIMO Systems. Authors used this scheme combine with two UL receiver detectors, maximum ratio combiner (MRC) and ZF to reduce PC problem in Multi cell UL Ma-MIMO Systems by maximizing the minimum UL rate of the target cell's user. They considered the large-scale characteristics of the fading channel to reduce inter-cell interference at the target cell; formulated the pilot assignment as problem optimization and develop algorithm, to increase the throughput by reducing the inter-cell interference, PC and evaluated the performance of in terms of SINR as the number of receiver antennas per cell goes to infinity. They also compared the proposed schemes with the SPA and the conventional schemes as a function of the number of BS's antennas using the ZF and MRC as a linear detector.

Finally, They concluded that the EPA scheme is best pilot assignment scheme. It provides the best performance and least complexity. But the paper did not consider intra cell interference.

In [25] Abhishek Thakur and Ramesh Chandra Mishra proposed performance analysis of energy efficient MU Ma-MIMO system. Authors investigated the EE MU Ma-MIMO system performance assuming channel reciprocity error using precoding schemes like MR, ZF and PRF to reduce the PC and optimize the SE for different user density per cell. They analyzed the Bit error rate (BER), average harvested energy and achievable rate of Ma-MIMO under Rician fading channel without increasing the bandwidth and cell density. They evaluated the SE versus number of BS antennas with perfect CSI, FDD and TDD; SE versus the number of users and different PRFs for both precoding techniques and BER versus SNR (dB) for different smaller values of BS antennas. From the simulated result, They stated that BER is also negligible for small value of SNR.

By increasing number of antenna at BS, Ma- MIMO performance can be enhanced but there is some limit which is bounded by EE of the system, the deploying cost and circuit power consumption will increase and the achievable rate getting constant after some instant. so, the EE of the Ma-MIMO system will reduce. The SE performance in ZF is better than MR precoding because Ma-MIMO is noiseless communication system. TDD mode is showing better performance than FDD mode. For both ZF and MR precoding, $F=1$ is preferred when more number of users per cell is used and $F=7$ is preferred for less number of users per cell.

Then they concluded that the system performance found by assuming channel non reciprocal is lower than the performance by assuming that the channel is reciprocal, Frequency reuse factor can be increased when user density is less and vice versa for user's resource optimization and they obtained the SE of Ma-MIMO is 40 times more than the previous 4G network technology although the system is restricted to line of sight propagation.

In [26] Jun Zhang and Jun Zuo proposed Multi-Cell MU- Ma-MIMO Transmission with DL Training and PCP. Authors investigated the SE of beamforming training scheme with MRT precoding and derived closed-form expression of the SE to find the optimal lengths of UL and DL pilots. To improve the performance, they suggested the BT-PCP transmission scheme to minimize the PC interference with limited cooperation between BSs. The proposed BT-PCP scheme can significantly mitigate the PC interference when the number of BS antennas is large but still finite. They analyzed the SE achieved by the beamforming training scheme, and obtained the optimal lengths of pilot sequences

based on the derived approximate closed-form expression. The obtained results depicted that the performance gain due to CSI estimation at the user side but, the SE per cell in multi-cell is reduced because of PC as compare with single-cell scenario. Based on the observed result, They conclude that the proposed scheme provides better performance than the conventional PCP method, and the performance gap between the perfect CSI case and BT-PCP is small. But the analysis was focused on uncorrelated channel and used only MRT precoding

In [27] Qasim Jabbar and Yu Li suggested evaluation, analysis of performance Gains and Trade offs for Ma-MIMO Systems. Authors studied the system performance gains are in a multi-cell DL Ma-MIMO system under i.i.d Rayleigh fading channel model with both perfect and imperfect channel estimation and also the effect of interference among cells due to pilot sequences contamination. They evaluated and analyzed the performance of the Array and spatial multiplexing gain as a function of the number of antennas with both perfect and imperfect channel estimation with multi-cell system. Additionally, They studied these gains trade offs. They also analyzed comparison between Ma-MIMO and Conventional MIMO Systems in term of Outage Probability and from the simulation result, they obtained that Both the Array and the spatial multiplexing gain are increased with Ma-MIMO system as the number of antennas increases. Although the system performance is degraded with imperfect estimation due to the sharing of the same pilot sequences from users in other cells which it makes pollution in channel estimation.

They concluded that all gains cannot be maximized simultaneously.

Additionally, discussed the effect of pilot interference on the trade off between energy and spectral efficiency, this reduces the system performance and a comparison was made between imperfect and perfect CSI on array gain and multiplexing gain but They analyzed the system performance Gains in ideal case(i.e. assumed i.i.d Rayleigh fading channel model), considered unbounded number of antennas and used only MRT precoding.

In [28] Ukman Audah and Adeeb Salh suggested mitigating PC for Channel Estimation in Multi-cell Ma-MIMO Systems. Authors used a channel-estimation scheme by applying an orthogonal pilot reuse sequence to minimize PC in edge users with minimized channel quality as per the approximation of large-scale fading, and evaluated the performance of this scheme using the ZF and MRT precodings under the channel is i.i.d Rayleigh fading.

They described that largely interfering users in neighboring cells are determined according to large-scale fading estimation. These users are included in the joint channel processing. The Achievable data rate of ZF precoding technique gave better values than MRT as a function of different number of antennas and PRF of three and one. Additionally, the ZF precoding provides better data rate than the MRT precoding for large pilot reuse due to the ZF precoding could be applied at high SINR values. The data rate is increased when the number of edge users or the grouping parameter was fixed. channels became orthogonal to the other channels and reduces interference between neighboring cells as the numbers of antennas in the multi-cell system increased. The achievable data rate with respect to different number of users is better with ZF precoding than MRT precoding. This is due to massive number of pilot reuse sequences and the ZF precoding can minimize the inter-cell interference between neighboring cells became orthogonal to the other channels and restrained the interference between neighboring cells.

Finally, They generalized as system performance is improved using both MRT and ZF precoders with respect to the number of antennas and achievable data rate is maximized because of the orthogonal pilot reuse sequence in the DL improved estimation quality in the channel.

Even though the related works deal about the performances of multicell Ma-MIMO system either using linear precoding and non-linear precoding techniques or pilot assignment schemes, They did not consider performances of the multicell Ma-MIMO system for three precoding techniques such as ZF MRT, and MMSE and PRF and their comparison under practical channel model, spatially correlated Rayleigh fading channels.

This thesis focuses the performance analyze of multicell Ma-MIMO systems using MRT, ZF and MMSE precoding techniques combined with PRF under spatially correlated Rayleigh fading channel model and compare the performance of those precoding techniques with perfect CSI and the combination of precoding techniques with PRF (1,3 and 4) for the case of imperfect CSI in terms of the SE as a function of number of BS antennas and the SE with respect to number of users under different consideration.

System and Channel Model of DL

Ma-MIMO Systems

In this chapter we will see DL multi cell Ma-MIMO system, channel and signal model. Similarly, the mathematical expression of SINR and SE of the system with perfect and imperfect CSI will be derived with the three precoding techniques.

3.1 System Model

A Multi-Cell Ma-MIMO system involves multiple BSs with massive number of antennas serving different users in different cells. Each BS antennas work coherently together and different BSs do cooperate. the pilot sequence used in a particular cell is reused in other cells, and this results intercell interference. Assume the system works in synchronized operation, either all BSs simultaneously transmit or all user terminals simultaneously transmit at any given point in time. Ma-MIMO is a MU-MIMO system where a BS with a large number of antennas array simultaneously serve many user terminals. It has a great advantage in increasing spatial multiplexing gain (increased data rate) because the BS is equipped with many antennas and sends the independent data streams to many users simultaneously. Since the antennas generate a lot of communication paths where the radio signal can propagate over different paths, the link reliability can be enhanced and the SE will be improved because the BS is able to focus its transmission power into the spatial direction where each user is located (array gain). However, in multi-cell MU Ma-MIMO systems, there is PC problem. This is due to the user terminals use the same pilots while UL training to estimate the channel at the BS. Similarly, because of limited coherence block, the orthogonal pilot sequence is also limited. Thus, this pilots sequences reused in neighboring cells interfere with each other, and the obtained estimated channel in a given cell can be contaminated by pilots transmitted by users in other cells. This estimated

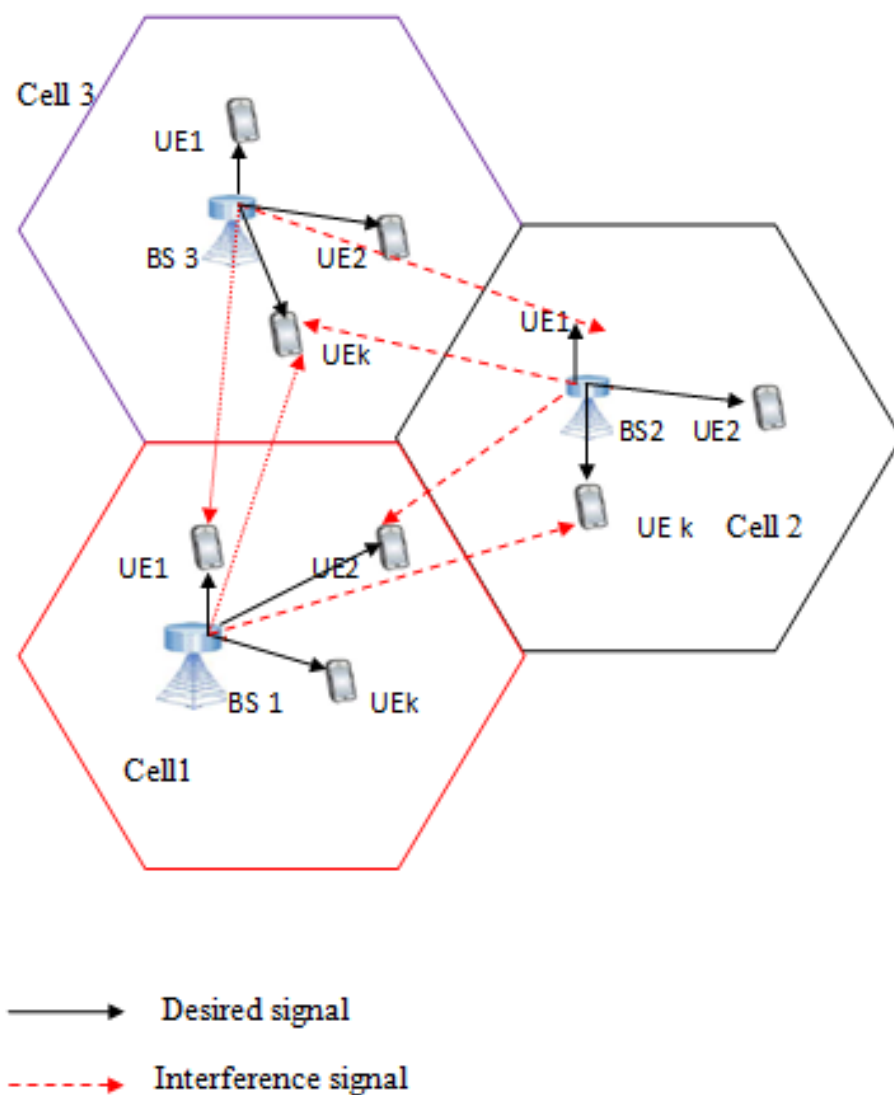


Figure 3.1: Three Cells Multi-user Downlink TDD-Massive MIMO System Model

channel is then used to transmit the DL data and finally it degrades the performance of the system. Precoding techniques are used to focus each signal at its desired user terminal and mitigate interference towards other terminals.

Figure 3.1 shows the Multi-Cell MU-DL TDD-Ma-MIMO system model. In this model, the system composed of L hexagonal cells, and each cell contains a BS with M -antennas and K single-antenna user terminals and in each cell, K single-antenna users communicate simultaneously to their BS, assuming that $M \gg K$.

3.2 Propagation Channel Model

Let h_{jk}^i is the channel response between user k in cell j and the BS in cell i , and this channel response represents the propagation channels of the k^{th} user located in the j^{th} cell and the BS in i^{th} cell and it is modeled as spatial correlated Rayleigh fading. The channel responses are all Gaussian distributed with zero mean and it is entirely defined through the correlation matrices [29]. Due to practical channels are generally spatially correlated, the BS antennas have non-uniform radiation patterns and the physical propagation environment makes some spatial directions more probable to carry strong signals from the transmitter to the receiver than other directions [12][29]. By considering path-loss, shadowing, multipath fading and spatial channel correlation, a correlated Rayleigh fading channel model of a user is expressed as [29]

$$h_{jk}^i \sim N_C(0, R_{jk}^i) \quad (3.1)$$

where N_C denotes complex Gaussian distribution. In which the channel response converges to complex Gaussian distribution.

$R_{jk}^i \in \mathbb{C}^M \times M$ is positive semi-definite spatial channel correlation matrix which represents the model for the large scale fading. Gaussian distribution is used to model the small-scale fading variations [3]. The spatial channel correlation matrix describes the macroscopic propagation effects including the radiation patterns and antenna gains at the transmitter and receiver. Thus, the average channel gain from the i^{th} BS antenna to user k in cell j is given by [3].

$$\beta_{jk}^i = \frac{1}{M} \text{tr}(R_{jk}^i) = \Upsilon - 10\alpha \log_{10} \frac{d_{jk}^i}{1 \text{ km}} + F_{jk}^i \quad (3.2)$$

where

β_{jk}^i the large-scale fading coefficient. That describes the effect of both path-loss and shadowing. d_{jk}^i is distance between the k^{th} user in the j cell and the BS in i^{th} cell and the receiver. α is the pathloss exponent. Υ is the median channel gain at the reference distance of 1 km. .

F_{jk}^i represents a log-normal shadowing, $F_{jk}^i \sim N(0, \sigma_{sh}^2)$ around the nominal value $\Upsilon + 10\alpha \log_{10} \frac{d_{jk}^i}{1 \text{ km}}$ where σ_{sh} is the standard deviation of the shadow fading model. The

shadow fading adds random correction term to obtain a model that better fits with practical channel measurements [12].

In a nutshell, channel models are either stochastic or deterministic [30]. Deterministic channel models depends on a given environment with fixed locations of transmitters, receivers, and scatterers . These models include deterministic LOS channel model, recorded channel measurements and ray tracing based on 3D-building models [31]. Although, deterministic channel models can provide very accurate performance predictions for specific scenarios, they are only valid for a specific scenario and thus they do not allow for comprehensive conclusions. Besides, due to very few openly accessible databases of channel measurements and 3D-building models, the results cannot be easily reproducible [12][30][32]. Stochastic channel models are used to generate a large number of channel realizations with desired statistical properties and are not depend on a particular environment. These models include correlation-based, geometry-based channel and parametric-based . Correlated based Rayleigh fading channel model is one of the correlation-based channel model. The channel responses are all Gaussian distributed with zero mean and it is entirely defined through the correlation matrices. Parametric channel models describes stochastic distributions of the number of multipath clusters and power, the delay profile, AoD and AoA of the individual multipath components [12][31]. This models are not depend on the geometry of the propagation environment, they are infeasible for system-level simulations of the channel with time-evolution that is caused by movements of the transmitters and receivers. A geometry-based stochastic channel models represents a distribution of the physical location of scatterers around the transmitters and receivers. Individual propagation paths are modeled in a quasi-deterministic manner; Once the locations of all scatterers are chosen. Such models are agree very well with measurements, easy to simulate, and enable time-evolution [12][31][32]. To simplify our analysis, we consider the local scattering based spatial channel correlation Model.

3.3 Local Scattering based Spatial Channel Correlation Model

The local scattering correlation model describes the basic characteristics of spatial channel correlation in terms of angular standard deviation (ASD) and the nominal angle. These are the basic parameters to model the spatial channel correlation matrix. The ASD describes the random deviation from the nominal angle with given standard deviation. The scenario of a Ma-MIMO system under NLOS propagation with the local scattering spatial correlation model is shown in Figure 3.2. This approach helps to develop a model

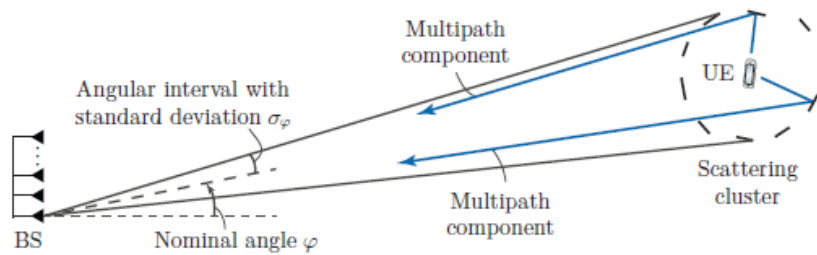


Figure 3.2: NLOS propagation under local scattering spatial correlation model [29]

for the spatial correlation matrix for NLOS propagation between the user and the BS equipped with uniform linear array (ULA) antennas. The received signal at the BS is the superposition of N -multipath components. Suppose the scattering is localized around the user and if there is no scatterers in near field of the BS, each of the multipath components results in a plane wave that reaches the array from a particular angle and gives an array response of [3].

$$\mathbf{a}_n = g_n \left[1 e^{j2\pi d_h \sin(\bar{\varphi}_n)} \dots e^{j2\pi d_h (M-1) \sin(\bar{\varphi}_n)} \right]^T \quad (3.3)$$

where $\mathbf{a}_n \in \mathbb{C}^M$, $g_n \in \mathbb{C}$ accounts for the gain and phase rotation for this path, φ_n is the arrival angle and d_h is the spacing between the BS antennas. The channel response at the BS is the superposition of multipath components and expressed as [28].

$$\mathbf{H} = \sum_{n=1}^N \mathbf{a}_n \quad (3.4)$$

when the arrival angles $\bar{\varphi}_n$ are iid random variable with angular probability density function of $f(\bar{\varphi}_n)$ and g_n are iid random variables with zero mean and variance of $\mathbb{E}\{|g_n|^2\}$

The variance describes the average channel gain of the n^{th} path and the total average gain of the multipath components is denoted by $\beta = \sum_{n=1}^N \mathbb{E} \{ |g_n|^2 \}$. When $N \rightarrow \infty$, by using the central limit theorem, the channel response converges to [3].

$$\mathbf{H} \rightarrow \mathbf{N}_C(0, \mathbf{R}) \quad (3.5)$$

where \mathbf{N}_C denotes complex Gaussian distribution. Besides, the spatial channel correlation is formulated as $\mathbf{R} = \mathbb{E} \{ \sum_n \mathbf{a}_n \mathbf{a}_n^H \}$ by using equation 3.3, the $(j, m)^{\text{th}}$ element of the spatial channel correlation can be expressed as [28]

$$\mathbf{R}_{jm} = \beta \int e^{j2\pi d_h(j-m) \sin(\bar{\varphi})} f(\bar{\varphi}) d\bar{\varphi} \quad (3.6)$$

As shown in equation 3.6, \mathbf{R}_{jm} depends on the difference $j-m$, hence \mathbf{R} is Toeplitz matrix. Assuming that all the multipath components originate from a scattering cluster localized around the user, at the BS antennas $\bar{\varphi} = \varphi + \delta$ where φ is the deterministic nominal angle and δ is the random deviation from the nominal angle with angular standard deviation σ_φ . The ASD is measured in radians and determines how large the deviation from the nominal angle. The random deviation can be modeled as Gaussian distributed, Laplace distributed and Uniformly distributed deviations [3][29].

But here, we assume the Gaussian angular standard distribution model. In Gaussian angular distribution with small ASD values, an approximate closed form expression of the spatial channel correlation matrix can be expressed as [29]

$$\mathbf{R}_{jm} = \beta e^{j2\pi d_h(j-m) \sin(\varphi)} e^{-\frac{\sigma_\varphi^2}{2} j2\pi d_h(j-m) \cos(\varphi)^2} \quad (3.7)$$

This approximation helps to reduce the computational complexity and also gives some insights on the structure of the correlation matrix. When $\sigma_\varphi = 0$, $\mathbf{R}_{jm} = \beta e^{j2\pi d_h(j-m) \sin(\varphi)}$ and all multipath components arrive from angle φ and gives rank-one correlation matrix. Whereas, for $\sigma_\varphi > 0$ the diagonal elements are the same, but off-diagonal elements decrease with $e^{-\frac{\sigma_\varphi^2}{2} (2\pi d_h(j-m) \cos(\varphi))^2}$ and goes to zero as σ_φ grows to large [12].

3.4 Channel Estimation

The BS requires CSI in Mu-MIMO systems to separate the signals associated with the different users. Perfect CSI can not be achieved in practice, since the channels are changing over time and frequency, and thus must be estimated using limited resources. The channel estimation of a frequency-selective channel can be handled by splitting the frequency resources into multiple independent frequency-flat sub channels that can be estimated separately. A pilot sequence, which is known is transmitted over each such sub channel and the received signal is used to estimate the channel response. To explore all spatial channel dimensions, this sequence must at least have the same length as the number of BS antennas [8].(i.e. a pilot sequence sent by the BS needs to have the length M, while the combined pilot sequence sent by the single-antenna user terminals needs to have the length K.)

There are FDD and TDD modes of implementing the UL and DL transmission over a given frequency band. **In FDD** mode the bandwidth is split into two separate parts: for the DL and UL. Pilot sequences are needed in both the DL and UL due to the frequency selective fading, giving an average pilot length of $\frac{(M+K)}{2}$ per sub channel. DL CSI is estimated by the users and fed back to the BS. For a large number of BS antennas, CSI estimation and feedback may become very complex. For **TDD** mode the whole bandwidth is used for both DL and UL transmission, but separated in time.

Ma-MIMO uses TDD mode to estimate channel at the BS via UL pilots, which is preferred over FDD [11], it permits channel estimation in one side, UL and avoids the estimation of the other side, DL due to channel reciprocity property. This indicates that TDD based channel reciprocal reduces the overhead signals used for channel estimation and saves bandwidth of the system. In TDD, DL and UL channels are reciprocal due to this mode uses the same frequency spectrum for the DL and UL transmissions but with different time slots. It requires shorter pilots than FDD, but is also highly scalable since the pilot length is independent on the number of BS antennas. In practical system, due to hardware chains are mismatched, the DL and UL channels cannot be perfectly reciprocal. But with proper calibration [7], this non reciprocity can be removed. Here in this thesis work, the hardware chain calibration is assumed to be perfect.

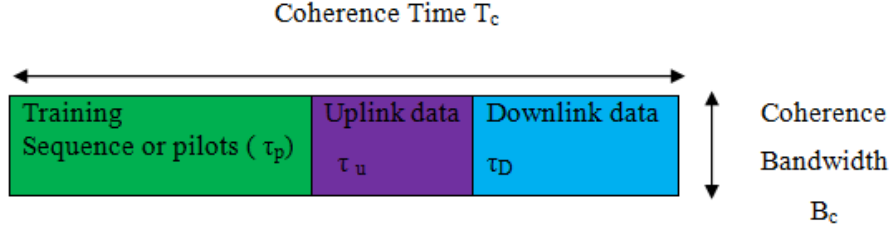


Figure 3.3: Time-division duplex Protocol [3]

A coherence block (τ_c) consists of a number of time samples and sub carriers over which the channel response can be approximated as constant and flat-fading. Each coherence block contains $\tau_c = B_c T_c$

where B_c is the coherence bandwidth and T_c is the coherence time. The DL transmission has two steps: Training step and DL data transmission step.

3.4.1 Uplink Training Phase (Uplink Pilot Transmission) Based Channel Estimation

In the training step, the BS estimates the CSI from K users that depends on the received pilot sequences in the UL so as to make efficient use of the massive number of antennas. Users transmit pilots to BSs, and then the BSs will estimate the corresponding channel coefficients. Let τ_p samples are reserved for UL pilot signaling or training phase in each coherence block. Each UE sends a pilot sequence that spans these τ_p samples. All user terminals in the system send pilot sequences to BSs synchronously, and then the i^{th} BS receives the pilot sequences transmitted from users and these received pilot sequences at the i^{th} BS is denoted by $Y_i^P \in \mathbb{C}^{M \times \tau_p}$ as shown in equation 3.8 [29]

$$Y_i^P = \sum_{k=1}^{K_i} \sqrt{\rho_{ik}} h_{ik}^i \phi_{ik}^H + \sum_{j=1, j \neq i}^L \sum_{m=1}^{K_j} \sqrt{\rho_{jm}} h_{j m}^i \phi_{jm}^H + N_i \quad (3.8)$$

where the superscript P in Y_i^P stands for pilots. p_{ik} is The UL transmit power which scales the elements of ϕ_{ik} . H is used as transpose. N_i denotes the additive white Gaussian noise (AWGN). The first term in equation 3.8 represents the received pilot signals from users in the home or target cell. The middle term express the inter-cell interference signal from the neighbor cells, which causes the pilot contamination.

The BS performs a de-spreading operation by correlating the received signals with each of the K pilot sequences. This is equivalent to right-multiplying the received signal matrix by the matrix of pilots, yielding [29].

$$Y_{ik}^i = \sqrt{\rho_{ik}} h_{ik}^i \phi_{ik}^H \phi_{ik}^* + \sum_{m=1, m \neq k}^{K_i} \sqrt{\rho_{im}} h_{im}^i \phi_{im}^H \phi_{ik}^* + \sum_{j=1, j \neq i}^L \sum_{m=1}^{K_j} \sqrt{\rho_{jm}} h_{jm}^i \phi_{jm}^H \phi_{ik}^* + N_i \phi_{ik}^* \quad (3.9)$$

The second and third terms in equation 3.9 represent interference and contain inner products of the form $\phi_{ik}^H \phi_{ik}^*$ between the pilot of the desired UE and the pilot of another UE i in cell j . To estimate the channel of a particular user, the BS needs to know the transmit pilot sequence of the user. so, the pilots should be deterministic sequences and pilot assignment is made when the user connects to the BS.

Ideally, all pilot sequences to be orthogonal, but practically, the pilots are limited, which, is τ_p -dimensional vectors due to coherence block is limited, for a given τ_p , we can only find a set of at most τ_p mutually orthogonal sequences. The limited length of the coherence blocks is limited, $\tau_p \tau_c$. Thus, assigning mutually orthogonal pilots to all UEs are impossible in practice. Assuming that the system uses a set of τ_p mutually orthogonal pilot sequences. These can be gathered as the columns of the UL pilot book $\phi \in \mathbb{C}^{\tau_p} \times \tau_p$ which satisfies $\Phi^H \phi = \tau_p I_p$.

For conventional pilot reusing scheme, the k^{th} users in all cells reuse the k^{th} pilot sequence, i.e. the set with the indices of all UEs use the same pilot sequence as UE k in cell i .

$$\rho_{ik} = \{(j, m) : \phi_{jm} = \phi_{ik}, \quad j = 1 \dots L, k = 1 \dots K_j \quad (3.10)$$

Equation 3.10 indicates UE m in cell j uses the same pilot as UE k in cell i , $(j, m) \in P_{ik}$ and Using then equation in 3.9 is simplified as:

$$Y_{ik}^i = \sqrt{\rho_{ik}} \tau_p h_{ik}^i + \sum_{(j, m) \in P_{ik} \setminus pik} \sqrt{\rho_{jm}} \tau_p h_{jm}^i + N_i \phi_{ik} \quad (3.11)$$

The first term in equation 3.11 represents the desired pilot signals. The second and third term describe interfering pilot and noise respectively. Where Y_{ik}^i is the processed received signal. The processed received signal is a sufficient statistics to estimate h_{jk}^i .

3.4.2 MMSE based Channel Estimation

In order to implement precoding and decoding, the home cell needs only an estimate of its own channel matrix. Assuming that the BS uses MMSE channel estimation.

The MMSE estimator of h_{jk}^i is the vector that minimizes the MSE $E \left\| h_{jk}^i - \hat{h}_{jk}^i \right\|^2$ where \hat{h}_{jk}^i is given as [29].

$$\hat{h}_{jk}^i = E \left\{ h_{jk}^i \mid Y_i^P \right\} = \sqrt{\rho_{jk}} R_{jk}^i \Psi_{jk}^i Y_{jk}^{i,P} \quad (3.12)$$

$$\Psi_{jk}^i = \sum_{j'r'k' \in pjk} \left(\sqrt{\rho_{j'r'k'}} \tau_p \{ R_{j'r'k'}^i + I_M \} \right)^{-1} \quad (3.13)$$

where φ_{jk}^i is the inverse of normalized correlation matrix. R_{jk}^i is the spatial correlation matrix of the channel to be estimated. $Y_{jk}^{i,P}$ is the received pilot sequences at the i^{th} BS that are transmitted from users in the j cells. The estimation error $\tilde{h}_{jk}^i = h_{jk}^i - \hat{h}_{jk}^i$ has the correlation matrix. The channel estimation quality can be determined by using the mean square error as $E \left\{ h_{jk}^i - \hat{h}_{jk}^i \right\} = \text{tr} \left(C_{jk}^i \right)$. In which a good estimation quality is represented by small MSE.

3.5 Pilot Contamination

Pilot contamination is caused by sharing of non-orthogonality of pilot sequences among users in adjacent cells, which is a crucial problem in Ma-MIMO [23]. It exists because of the practical necessity to reuse the time-frequency resources across cells. Each user terminals send UL pilot sequences to its BS simultaneously. This helps to know the channel responses of its user terminals. The BS needs to know the channel responses of its user terminals and these are estimated in the UL by sending pilot signals. Each pilot signal is corrupted by noise and inter-cell interference when received at the BS. For example, consider the scenario illustrated below where K number of user terminals are transmitting simultaneously, so that the BS receives a correlated of their pilot sequences. Thus, the desired pilot signal is contaminated. When estimating the channel from the desired terminals in a home cell(served cell), the BS cannot easily separate the transmitted pilot sequences from the all terminals. This has two basic indications:

- First, the interfering pilot sequences reduces the channel estimation quality.
- Second, the BS unintentionally estimates a superposition of the channel from the required terminals and from the interferes. as a result, the estimated channel at the BS is contaminated. This degrades the estimation quality.

Later, the desired terminals transmit payload data and the BS wishes to coherently combine the received signals, using the channel estimate. It will then unintentionally and coherently combine part of the interfering signal as well. This is particularly poisonous when the BS has M antennas, since the array gain from the receive combining increases both the signal and the interference power proportionally to M . Similarly, in DL transmission when the BS transmits a beam formed DL signal towards its terminal, it will unintentionally direct some of the signals towards to interferes. at the end, the system performance is degraded [23].

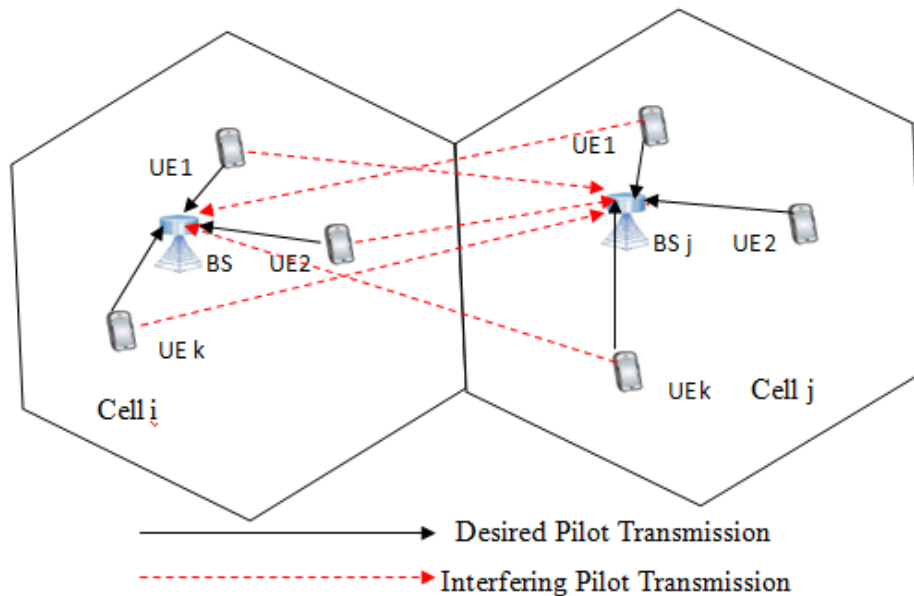


Figure 3.4: Uplink Pilot Contamination in a multi cell scenario where BS i in cell i receive pilots from adjacent cell [23]

3.6 Perfect and Imperfect CSIT

3.6.1 Perfect CSIT

Perfect CSIT means the channel is perfect, channel estimation is not required. That means all the components of H is known at the transmitter instantaneously and without errors i.e $E \{h_{jk}^i\} = E \{\hat{h}_{jk}^i\}$ [27]. The performance of the system can be increased very much using the CSIT in an ideal scenario. but this isn't achieved in real condition. in fact, perfect CSIT is impossible to achieve because the precision of the electronics should be infinite, the transmission should be instantaneous, and some other hypothesis that in the reality are impossible.

3.6.2 Imperfect CSIT

Perfect CSI can typically not be achieved in practice and to analyze the system performance in realistic, the CSI is incomplete [28]. It means that only a part of the channel is unknown. It can be due to some user not knowing its channel. Then a whole row of H_j^i is missing. Or due to some resources constraints in the system that does n't let know a specific amount of information of the channel. It can also be originated because a quantification error or an error on the obtainment of CSI. Using statistical properties, the missing information can be obtained.

3.7 Pilot Reuse Factor

In order to mitigate the PC, consider arbitrary pilot allocation with the only requirement of $\tau_p \geq K$ [33]. The parameter $N = \frac{\tau_p}{K} \geq 1$ is called the PRF. Full pilot reuse results to high inter-cell interference during channel estimation, that can be minimized using pilot reuse factor. PRF is designed to have each cell within a cluster to use unique orthogonal signals. This helps to mitigate inter-pilot contamination effect. It is calculated in a

similar manner to the cellular frequency reuse factor [33] given as:

$$N = i^2 + ij + j^2 \quad (3.14)$$

where i and j are positive integers

From equation 3.14 the possible PRF values are:1,3,4,7,9,12..

It is analogous to traditional frequency reuse. terminals within the pilot reuse area

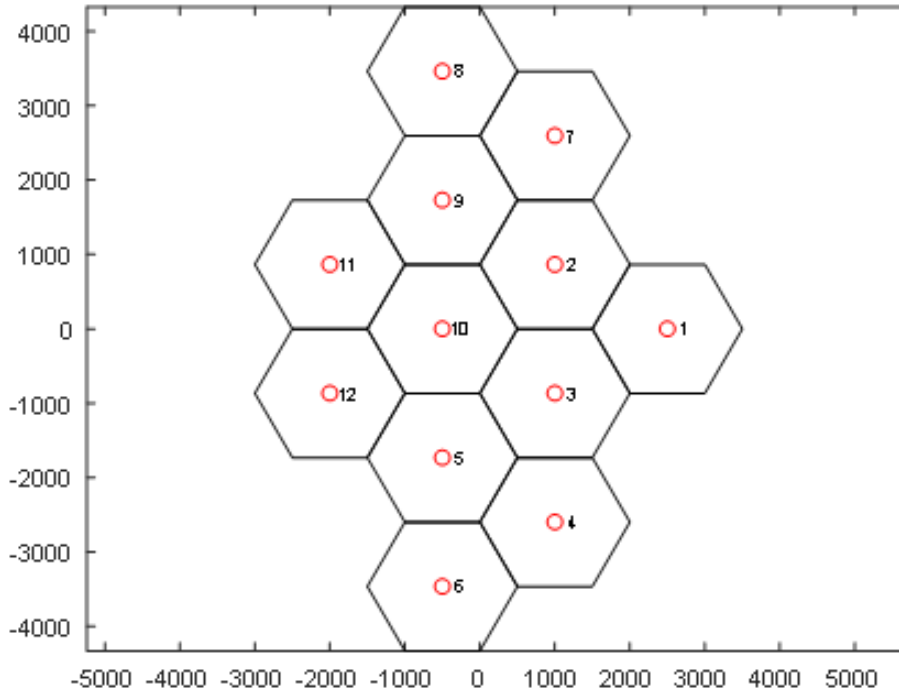


Figure 3.5: Cellular hexagonal cell with $N=3$ [3]

are confined to utilize only a fraction of the time-frequency resources during the channel estimation phase. However, with pilot reuse, each terminal is free to use all the available resources for data transmission during the rest of the coherence interval. The PRF $1/N$ is the rate at which pilot resources may be reused in the network.

Where N is the number of cells that are assigned orthogonal pilots. A factor N reduces the pilot contamination effect by assigning orthogonal pilots to neighboring cells, the next-neighbor cells and so on. The total number of pilots reserved for pilot transmission are $\tau_p = KN$,

where K is the number of users per cell.

Figure 3.5 and 3.6 shows a hexagonal geometric arrangement of cells with a PRF $N=3$ and 4. Each cell within a cluster is assigned unique orthogonal signals: 1, 2, 3 for a PRF $N=3$ and 1, 2,3, 4 for a PRF $N=4$. We assumed that every cell served exactly K

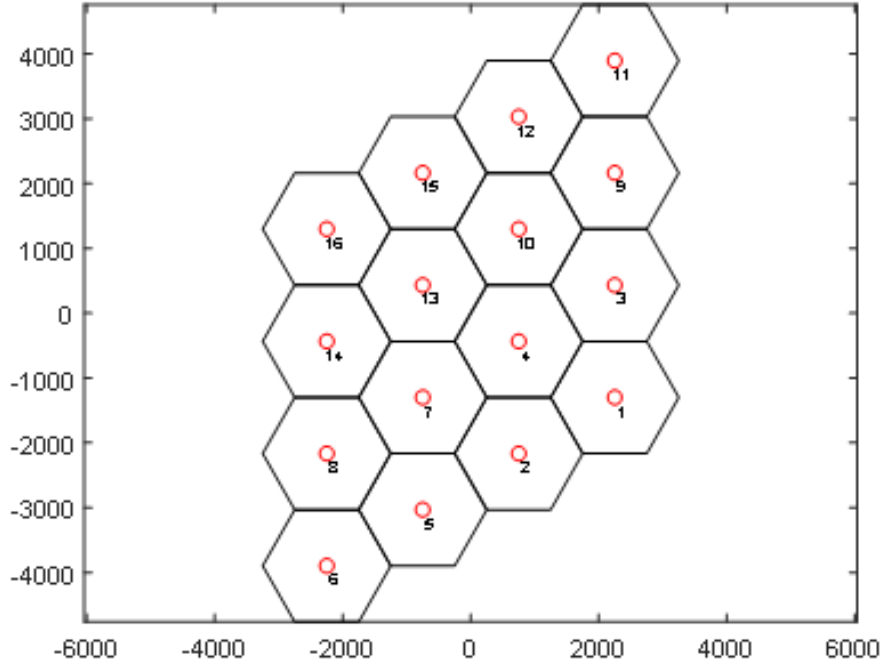


Figure 3.6: Cellular hexagonal cell with $N=4$ [3]

terminals; the minimum required duration of the pilot sequences is τ_p , would be equal to KN . For each of the N groups of pilots, $i = 1, \dots, N$, denote by $K_{max, i}$ the maximum number of terminals served by any of the cells in that group. Then the required pilot duration is equal to the total number of mutually orthogonal pilots in the system.

$$T_P = \sum_{i=1}^N K_{max} \cdot i \quad (3.15)$$

Each terminal in a cell is randomly assigned one of the pilot sequences allocated to that cell. The reuse factor should divide the total number of cells. The cells are enumerated such that the n^{th} cell and the $(n \pm N)^{\text{th}}$ cell use the same set of orthogonal pilots.

3.8 Signal Model of Downlink Data Transmission

3.8.1 DL Data Transmission

The BS has to ensure that each terminal receives only the signal intended for it. DL data transmission uses a linear precoding operation that combines data symbols with the channel estimates to create the actual signals that the array transmits. The j^{th} BS in cell j independently transmitting a signal, X_j [30].

$$X_j = \sum_{m=1}^{K_j} A_{jm} S_{jm} \quad (3.16)$$

where A_{jk} is the precoding vector that determines the spatial directivity of the transmis-

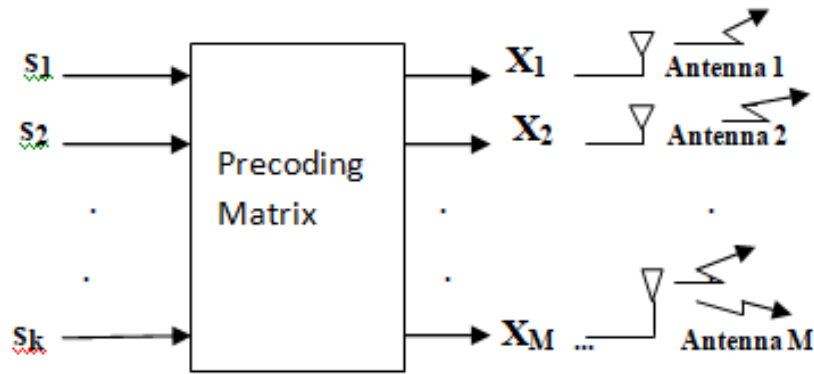


Figure 3.7: Block diagram of the linear precoder at each BS [3]

sion. $S_{jk} \sim C_N(0, \rho_{jk})$ is a vector of K symbols intended for the K terminals in the cell. ρ_{jk} is the signal power. The average precoding vector is assumed to be unity. that is: $E\{\|A_{jk}\|^2\} = 1$, Such that $E\{\|A_{jk}S_{jk}\|^2\} = \rho_{jk}$, is the transmit power allocated to this UE. Users in the i^{th} cell received signal is defined as [3]:

$$Y_i = \sum_{j=1}^L (H_i^j)^H X_j + N_i \quad (3.17)$$

where $\mathbf{N}_i = [n_{i1}, n_{i2} \dots n_{ik}]^T \in \mathbb{C}^K$ is the noise vector of the k user in cell i. Each users received DL signal in cell i can be written as

$$Y_{ik} = (\mathbf{h}_{ik}^i)^H \mathbf{A}_{ik} S_{ik} + \sum_{m=1, k \neq m}^{K_i} (\mathbf{h}_{ik}^i)^H \mathbf{A}_{im} S_{im} + \sum_{j=1, j \neq i}^{K_j} \sum_{m=1}^{K_j} (\mathbf{h}_{ik}^j)^H \mathbf{A}_{jm} S_{jm} + N_{ik} \quad (3.18)$$

Where \mathbf{A}_{jm} is the m^{th} column of precoding matrix \mathbf{A}_j . Equation 3.18 represents the de-

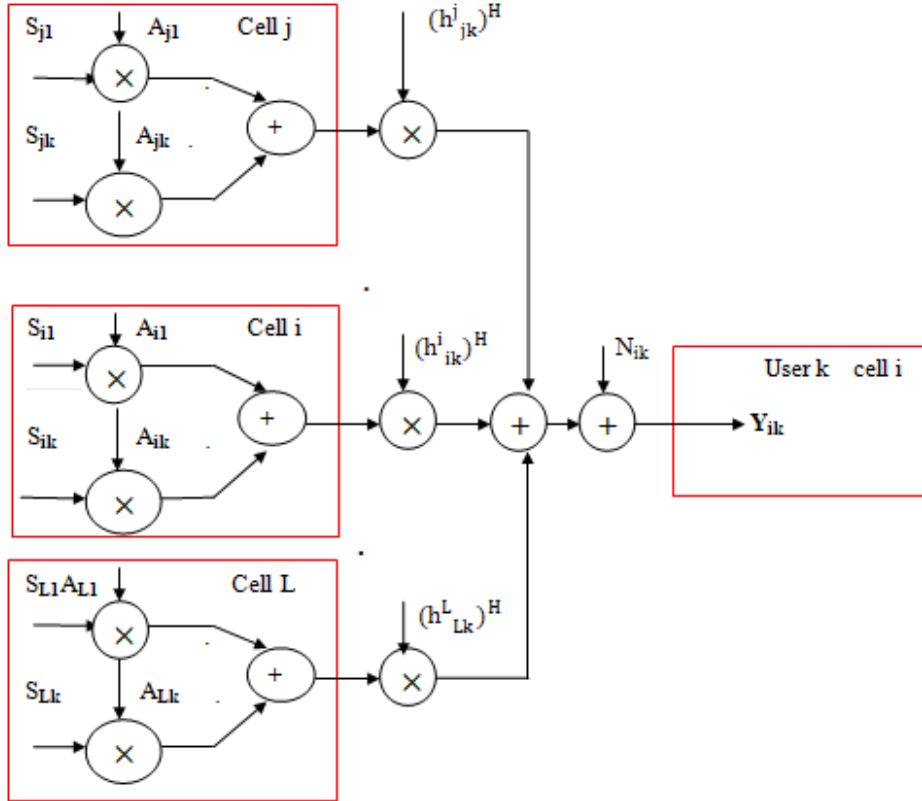


Figure 3.8: : Block diagram representation of a multi-cell DL Ma-MIMO system with linear precoding [3]

sired signal for the user k in cell i, intra-cell interference signal, and inter-cell interference signal, respectively.

3.9 Precoding Techniques

Transmit precoding is a generalization of beamforming to support multi-stream transmission in multi-antenna wireless communications. It is a versatile technique for signal

transmission from an array of M antennas to one or multiple users. In wireless communications, its goal is to increase the signal power at the intended user and reduce interference to non-intended users. A high signal power is achieved by transmitting the same data signal from all antennas, but with different phases and amplitudes such that the signal components add coherently at the user. Low interference is accomplished by making the signal components add destructively at non-intended users. This corresponds mathematically to designing beamforming vectors (that express the phases and amplitudes) to have large inner products with the vectors describing small inner products with non-intended user channels and the intended channels. Since transmit precoding focuses the signal energy at certain places, less energy arrives to other places because it permits SDMA, which is K spatially separated users are served simultaneously.

In Ma-MIMO systems, space division multiple access (SDMA) is implemented using a precoder. There are two types of precoding techniques. These are:

- Non-linear and
- Linear precoding.

1. Nonlinear Precoding Techniques

Nonlinear Precodings Provide better performance than linear precodings. These include Dirty Paper Coding (DPC), THP, etc.. and these precodings have the ability to achieve Shannon capacity [34] although with a huge computational complexity and are difficult to implement in real systems, like MIMO systems. In fact, nonlinear precoding techniques are vital important when M is not much larger than K , which is not the case in Ma-MIMO. Thus, linear precoding techniques are chosen in Ma-MIMO due to low complexity.

2. Linear Precoding Techniques

Linear Precoding has lower performance prove their ability to approach near capacity with low computational complexity. These linear precoding techniques include MRT, MMSE, ZF, RZF and etc [35].

The three linear precoding techniques like MRT, MMSE and ZF are used to reduce the inter user interference or intra cell interference for both perfect and imperfect CSI in this thesis work.

MRT precoding is the DL version of maximum ratio combining of the UL. MRT is

a pre-processing technique at the transmitter. It maximizes signal gain at the intended user [27].

ZF precoding: ZF precoding is a type of precoding technique, which eliminates the interference by transmitting the signal toward the intended user while nulling in the directions of other users. It is the pseudo-inverse of the CSI matrix.

MMSE Precoding: MMSE tries to strike a balance between getting the most signal amplification and reducing the interference.

3.10 Spectral Efficiency with Perfect and Imperfect CSI

Performance is one of the main factors, which is required for any communication network. It represents the measure of quality of the service provided by wireless communication network. These performance metrics also help us to discover original drifts and proactively respond to performance issues. The system performance can be defined by several methods. Among these methods, the SE is one of the method to measure the system performance. It is the amount of information transferred per second over a unit bandwidth. The SE is followed by Shannon theorem. This theorem describes the maximum rate in which the transmitter can transmit over the channel.

3.10.1 Spectral Efficiency with Perfect CSI

In perfect CSI, channel estimation is not required. Hence, the pilot sequences received from the users aren't required because the BS knows the propagation channel matrix H_i^i of multi cell Ma-MIMO system. the precoding matrix is described in terms of propagation channel matrix H_i^i [27]. Assume the scaling factor of precoding vector is unity.

$$\begin{aligned}
 A_i^{\text{MRT}} &= (H_i^i)^H, \quad \text{MRT Precoding} \\
 A_i^{\text{ZF}} &= (H_i^i)^H \left(H_i^i (H_i^i)^H \right)^{-1}, \quad \text{ZF Precoding} \\
 A_i^{\text{MMSE}} &= (H_i^i)^H \left[\left(H_i^i (H_i^i)^H + K\sigma^2 p^{-1} \right)^{-1} \right], \quad \text{MMSE Precoding}
 \end{aligned} \tag{3.19}$$

where

$$A_i^{\text{MRT}} = [A_{i1}^{\text{MRT}} \quad A_{i2}^{\text{MRT}}, \dots, A_{ik}^{\text{MRT}}]$$

$$A_i^{\text{ZF}} = [A_{i1}^{\text{ZF}} \quad A_{i2}^{\text{ZF}}, \dots, A_{ik}^{\text{ZF}}]$$

$$A_i^{\text{MMSE}} = [A_{i1}^{\text{MMSE}}, A_{i2}^{\text{MMSE}}, \dots, A_{ik}^{\text{MMSE}}]$$

These are the three precoding matrix such as: MRT, ZF and MMSE expression of all K users in cell i. Since the channel is perfect, users will receive the desirable data transmission from their BS without interfering with other users from other cells. i.e. there is no inter-cell interference but there is inter user interference for finite number of antennas. Thus, assuming the system is behaving as a single cell [27].

Then by considering the expression in equation 3.18 above, the SINR of kth user in the cell i for perfect CSI can be evaluated as follows [27]:

$$\text{SINR}_{ik}^{\text{Perf, CSI}} = \frac{\rho_{ik} |A_{ik}(h_{ik}^i)^H|^2}{\sum_{m'=1, k \neq m}^K \rho_{im'} |A_{im'}(h_{ik}^i)^H|^2 + \sigma_n^2} \quad (3.20)$$

The SE for kth user in i cell and sum SE for ith cell is given as shown below in equation 3.21 and 3.22 respectively.

$$\text{SE}_{ik}^{\text{Perf, CSI}} = \log_2 (1 + \text{SINR}_{ik}^{\text{Perf, CSI}}) [\text{bit/s/Hz}] \quad (3.21)$$

$$\text{SE}_i^{\text{Perf, CSI}} = \sum_{k=1}^K \text{SE}_{ik}^{\text{Perf, CSI}} [\text{bit/s/Hz/cell}] \quad (3.22)$$

The SE of the system for perfect CSI is calculated using the three precoding techniques. **MRT precoding** is a pre-processing technique at the transmitter. It maximizes signal gain at the intended user. The normalized MRT Precoding matrix A_i^{MRT} can be obtained by the complex conjugate of the CSI matrix A_{MRT} and normalization factor α^{MRT} [27].

$$A_i^{\text{MRT}} = \alpha^{\text{MRT}} A_i \quad (3.23)$$

Assume that the normalization factor is unity (i.e. $\alpha^{\text{MRT}} = 1$). Thus, the A_i^{MRT} can be expressed in terms of channel matrix

$$A_i^{\text{MRT}} = (H_i^i)^H \quad (3.24)$$

and the k^{th} user of MRT precoding is A_i^{MRT} and its expressed as

$$A_{ik}^{\text{MRT}} = \left(h_{ik}^i \right)^H \quad (3.25)$$

Then the k^{th} user SINR and SE of MRT are expressed respectively as follows

$$\text{SINR}_{ik}^{\text{MRT Perf,CSI}} = \frac{\rho_{ik} \left| h_{ik}^i \right|^4}{\sum_{m'=1, k \neq m}^K \rho_{im} \left| h_{im}^i \left(h_{ik}^i \right)^H \right|^2 + \sigma_n^2} \quad (3.26)$$

$$\text{SE}_{ik}^{\text{MRT Perf,CSI}} = \log_2 \left(1 + \text{SINR}_{ik}^{\text{MRT Perf,CSI}} \right) \quad (3.27)$$

ZF is the pseudo-inverse of the CSI matrix. The k^{th} user of Zero forcing precoding is A_{ik}^{ZF} and its expressed as [27]:

$$A_{ik}^{\text{ZF}} = \left(h_{ik}^i \right)^H \left(h_{iki} \left(h_{ik}^i \right)^H \right)^{-1} \quad (3.28)$$

Then the k^{th} user SINR and SE of ZF are expressed respectively as follow:

$$\text{SINR}_{ik}^{\text{ZF Perf,CSI}} = \frac{\rho_{ik} \left| h_{ik}^i A_{ik}^{\text{ZF}} \right|^2}{\sigma_n^2} \quad (3.29)$$

$$\text{SE}_{ik}^{\text{ZF Perf,CSI}} = \log_2 \left(1 + \frac{\rho_{ik} \left| h_{ik}^i A_{ik}^{\text{ZF}} \right|^2}{\sigma_n^2} \right) \quad (3.30)$$

MMSE reduces the interference and improves the performance by minimizing the mean square error. This technique is generated by the mean square error method [27].

$$A_{ik}^{\text{MMSE}} = \left(h_{ik}^i \right)^H \left[\left(h_{iki} \left(h_{ik}^i \right)^H + K \sigma^2 p_{ik}^{-1} \right)^{-1} \right]. \quad (3.31)$$

Where K is the number of users. p_{ik} is the power allocated to k^{th} user. σ^2 is the noise variance

$$\text{SE}_{ik}^{\text{MMSE Perf,CSI}} = \log_2 \left(1 + \frac{\rho_{ik} \left| h_{ik}^i A_{ik}^{\text{MMSE}} \right|^2}{\sum_{m=1, k \neq m}^K \rho_{im} \left| A_{im} \left(h_{ik}^i \right)^H \right|^2 + \sigma_n^2} \right) \quad (3.32)$$

Where

$$\text{SINR}_{\text{ik}}^{\text{MMSE Perf, CSI}} = \frac{\rho_{ik} |h_{\text{ik}}^{\text{MMSE}}|^2}{\sum_{m=1, k \neq m}^K \rho_{im} |A_{\text{im}}(h_{\text{ik}}^{\text{MMSE}})^{\text{H}}|^2 + \sigma_n^2}$$

3.10.2 Spectral Efficiency with Imperfect CSI

In order to utilize the advantages of Ma-Mu-MIMO, accurate CSI is required at the BS. In multi-cell system, there is reused of pilots by users while user terminals send UL pilots to the BS to estimate the channel response within cell due to the coherence block is limited. If each cell is serving the maximum number of terminals, then the received pilot signals at the BS are contaminated by pilots transmitted by terminals in other cells. Therefore, the user in the i^{th} cell for example receives signal from its BS and from other BSs [28]. In imperfect CSI, there is estimation error because the transmitter not knows all the components of H_j^i . That is $[\text{tr}(C_j^i)] \neq 0$, i.e $E\{h_{jk}^i\} \neq E\{\hat{h}_{jk}^i\}$

The channel estimation error, $\tilde{h}_{jk}^i = h_{jk}^i - \hat{h}_{jk}^i$ and the channel vector, h_{jk}^i is expressed as [29]

$$h_{jk}^i = \tilde{h}_{jk}^i + \hat{h}_{jk}^i \quad (3.33)$$

Substitute the expression in equation 3.16 into 3.18 then the received DL signal vector by user k in cell i for imperfect CSI can be obtained

$$Y_{ik} = (\hat{h}_{ik}^i)^{\text{H}} A_{ik} S_{ik} + \sum_{m=1, k \neq m}^K (\hat{h}_{ik}^i) A_{im} S_{im} + \sum_{j=1, j \neq i}^L \sum_{m=1, k \neq m}^K (\hat{h}_{ik}^j) A_{jm} S_{jm} + \sum_{j=1}^L \sum_{m=1}^K (\tilde{h}_{ik}^j) A_{jm} S_{jm} + N_{ik} \quad (3.34)$$

The first term of equation 3.34 contains the intended signal, whereas the other three terms represent effective noise, including intra-cell and inter-cell interference due to non-orthogonal channels, interference from estimation error of DL effective channel, and receiver noise, respectively. Since we use TDD mode (UL pilot) that limits the pilot overhead, no DL pilots and we depend on instead on channel hardening. Thus, the users do not know their instantaneous channel realizations. However, they can learn their average equivalent channels, $E\{(h_{ik}^i)^{\text{H}} A_{ik}\}$. (i.e. without beamforming training, the users detect the signals based on the statistical CSI).

The DL signal vector received by user k in cell i for imperfect CSI in equation 3.34 or in

3.18 can then be expressed as [3]:

$$Y_{ik} = E \left\{ \left(h_{ik}^i \right)^H A_{ik} \right\} S_{ik} + \left(\left(h_{ik}^i \right)^H A_{ik} - E \left\{ \left(h_{ik}^i \right)^H A_{ik} \right\} \right) S_{ik} + \sum_{m=1, k \neq m}^K \left(h_{ik}^i \right)^H A_{im} S_{im} + \sum_{j=1, j \neq i}^L \sum_{m=1, k \neq m}^K \left(h_{ik}^j \right)^H A_{jm} S_{jm} + N_{ik} \quad (3.35)$$

The second term describes receiver's lack of knowledge about H. The first term in equation 3.35 is the desired signal received over the deterministic average precoded channel $\hat{h}_{jk}^i A_{ik}$, where as the remaining terms are random variables with realizations that are unknown to the UE.

The SINR and SE for k^{th} user in i cell for imperfect CSI in equation 3.34 and 3.35 are re-expressed as follow in equation 3.36 and equation 3.37, respectively.

$$\text{SINR}_{ik}^{\text{Imperf,CSI}} = \frac{\rho_{ik} \left| E \left\{ \left(A_{ik} \right)^H \right\} h_{ik}^i \right|^2}{\sum_{j=1}^L \sum_{m=1}^K \rho_{jm} \left| E \left\{ \left(A_{jm} \right)^H h_{ik}^j \right\} \right|^2 - \rho_{ik} \left| E \left\{ \left(A_{ik} \right)^H \right\} h_{ik}^i \right|^2 + \sigma_n^2} \quad (3.36)$$

$$\text{SE}_{ik}^{\text{Imperf,CSI}} = \left(\frac{\tau_d}{\tau_c} \right) \log_2 \left(1 + \text{SINR}_{ik}^{\text{Imperf,CSI}} \right) [\text{bit/s/Hz}] \quad (3.37)$$

Equation 3.36 is the lower bounded DL ergodic channel capacity of UE k in cell i

The SE expression can be expressed for any channel model and precoding scheme.

Where The expectations are with respect to the channel realizations.

$h_{jk}^i = \tilde{h}_{jk}^i + \hat{h}_{jk}^i$ and $E(\tilde{h}_{jk}^i \hat{h}_{jk}^i) = 0$. Due to the estimate and the estimation error are independent and have zero mean.

Where $\frac{\tau_d}{\tau_c}$ is the prelog factor, which is fraction of all samples used for DL data. It is also represent the ratio of the time needed in sending data to the coherence interval and describes the pilot overhead. It is equivalent to $1 - \left(\frac{\tau_p}{\tau_c} \right)$.

Equation 3.37 is re-write equivalent to in equation 3.38

$$\text{SE}_{ik}^{\text{Imperf,CSI}} = \left(1 - \left(\frac{\tau_p}{\tau_c} \right) \right) \log_2 \left(1 + \text{SINR}_{ik}^{\text{Imperf,CSI}} \right) [\text{bit/s/Hz}] \quad (3.38)$$

The sum SE for imperfect CSI of i^{th} cell is

$$\text{SE}_i^{\text{Imperf,CSI}} = E \left(\sum_{k=1}^K \text{SE}_{ik}^{\text{Imperf,CSI}} [\text{bit/s/Hz/cell}] \right) \quad (3.39)$$

We also used Linear precoding techniques such as MR, ZF and M-MMSE to analyze the performance of multicell Ma-MIMO systems with imperfect CSI. These Linear precoding techniques are selected using the UL-DL duality precoding design principle. The UL-DL duality theorem describes that the SE achieved in the UL can be achieved also in the DL, if the UL combining vectors are used as DL precoding vectors. i.e. if the DL power is allocated in a particular way based on the UL powers and the precoding vectors are selected based on the detection vectors [36]. Hence, under imperfect CSI, the DL precoding vectors are based on the UL receive combining vectors are expressed as follow [29]:

$$A_{ik} = \frac{V_{ik}}{\sqrt{Y_{ik}}} \quad (3.40)$$

where

$$Y_{ik} = \sqrt{E \{ \|V_{ik}\|^2 \}}$$

$$V_i = [V_{i1} \dots V_{ik}] = \begin{cases} V_i^{\text{MRC}} & \text{with MR precoding} \\ V_i^{\text{ZF}} & \text{with ZF precoding} \\ V_i^{\text{M-MMSE}} & \text{with M - MMSE precoding} \end{cases}$$

Equation 3.40 can be normalized by $\|V_{ik}\|$ instead of $\sqrt{E \{ \|V_{ik}\|^2 \}}$ to reduce variations in precoded channel $(h_{ik}^i)^H A_{ik}$.

$$V_i^{\text{MRC}} = \hat{H}_i^i$$

$$V_i^{\text{ZF}} = \hat{H}_i^i \left(\left((\hat{H}_i^i)^H \right) \hat{H}_i^i \right)^{-1}$$

$$V_i^{\text{M-MMSE}} = \left(\sum_{j=1}^L \hat{H}_j^i P_j \left(\hat{H}_j^i \right)^H + \sum_{j=1}^L \sum_{m=1}^{K_j} P_{jm} C_{jm}^i + \sigma_{\text{UL}}^2 \mathbf{I}_M \right)^{-1} \hat{H}_i^i P_i$$

MRT Precoding Techniques

It is a linear precoding technique that maximizes the SINR. The MRT precoding for UE k in cell i is determined based on the channel estimate, h_{ik}^i or the UL receive combining vectors, $V_{ik}^{\text{MRC}} = \hat{h}_{ik}^i$ [29].

$$A_{ik} = \frac{\hat{h}_{ik}^i}{\sqrt{Y_{ik}}} \quad (3.41)$$

The precoding normalization constraint is assumed to be unity. that is: $E \{ \|A_{ik}\| \} = 1$
The SE can be calculated in closed form for this average-normalized MRT precoding.

The SE of average-normalized MRT precoding is expressed as [29]: $A_{ik} = \frac{\hat{h}_{ik}^i}{\sqrt{E\{\|\hat{h}_{ik}^i\|^2\}}}$

$$SE_{ik}^{\text{MRT}} = \left(\frac{\tau_d}{\tau_c}\right) \log_2 \left(1 + \text{SINR}_{ik}^{\text{Imp CSI, MRT}}\right) [\text{bit/s/Hz}] \quad (3.42)$$

ZF Precoding Techniques ZF precoding is linear precoding technique that is used to cancel the intra-cell interference. This precoding is a normalization of ZF combining vector. The ZF combining vector is assumed to implement a pseudo-inverse of the estimated channel matrix [36].

$$\mathbf{A}_{ik}^{\text{ZF}} = \frac{\mathbf{V}_{ik}^{\text{ZF}}}{\|\mathbf{V}_{ik}^{\text{ZF}}\|} \quad (3.43)$$

where $\mathbf{V}_{ik}^{\text{ZF}} = \hat{\mathbf{H}}_i^i \left((\hat{\mathbf{H}}_i^i)^H \hat{\mathbf{H}}_i^i \right)^{-1}$, the ZF combining vector. The SE expression of average-normalized ZF precoding, with $A_{ik} = \frac{\hat{h}_{ik}^i \left(\hat{h}_{ik}^i \hat{h}_{ik}^{iH} \right)^{-1}}{\sqrt{E\{\|\hat{h}_{ik}^i \left(\hat{h}_{ik}^i \hat{h}_{ik}^{iH} \right)^{-1}\|^2\}}} = \frac{\mathbf{V}_{ik}^{\text{ZF}}}{\|\mathbf{V}_{ik}^{\text{ZF}}\|}$ and based on the MMSE channel estimate [29].

$$SE_{ik}^{\text{ZF}} = \left(\frac{\tau_d}{\tau_c}\right) \log_2 \left(1 + \text{SINR}_{ik}^{\text{Imp CSI, ZF}}\right) [\text{bit/s/Hz}] \quad (3.44)$$

M- MMSE Precoding Techniques

The multi-cell MMSE precoding matrix of cell i is expressed based on the multi-cell MMSE receive detector matrix of cell i [29][36].

$$\mathbf{A}_i^{\text{M-MMSE}} = \frac{\mathbf{V}_i^{\text{M-MMSE}}}{\|\mathbf{V}_i^{\text{M-MMSE}}\|} \quad (3.45)$$

where,

$$\mathbf{V}_i^{\text{M-MMSE}} = [\mathbf{V}_{i1} \mathbf{V}_{i2} \dots \mathbf{V}_{iK}] = \left(\sum_{j=1}^L \hat{\mathbf{H}}_j^i \mathbf{P}_j \left(\hat{\mathbf{H}}_j^i \right)^H + \sum_{j=1}^L \sum_{m=1}^{K_j} P_{jm} \mathbf{C}_{jm}^i \right) + \sigma_{\text{UL}}^2 \mathbf{I}_M \Big)^{-1} \hat{\mathbf{H}}_i^i \mathbf{P}_i$$

$\mathbf{P}_i = \text{diag}(p_{j1}, p_{j2}, \dots, p_{jK})$ is the transmit powers of all UEs in cell j.

$\hat{\mathbf{H}}_j^i$ is estimated channel matrix that containing the estimates of all channels from UEs in cell j to BS i.

The multi-cell MMSE precoding vector of k^{th} user in i^{th} cell is expressed based on the multi-cell MMSE combining vector of k^{th} user in i^{th} cell.

$$\mathbf{A}_{ik}^{\text{M-MMSE}} = \frac{\mathbf{V}_{ik}^{\text{M-MMSE}}}{\|\mathbf{V}_{ik}^{\text{M-MMSE}}\|} \quad (3.46)$$

$$\text{SE}_{\text{ik}}^{\text{M-MMSE}} = \left(\frac{\tau_{\text{d}}}{\tau_{\text{c}}} \right) \log_2 \left(1 + \text{SINR}_{\text{ik}}^{\text{Imp CSI, M-MMSE}} \right) [\text{bit/s/Hz}] \quad (3.47)$$

M-MMSE combining maximizes the instantaneous SINR and also minimizes the MSE in the data detection; which is, the average squared distance between the desired signal and the processed received signal.

Simulation Results and Discussion

In this chapter, we will present the simulation results, and analysis for the performance analysis of the system.

4.1 Simulation setup

The system performance evaluations are analyzed for five different cases.

Case 1. SE performance evaluation (analysis) using PRFs and linear precoding techniques at different BS number of antennas with imperfect CSI.

Case 2. SE performance analysis using linear precoding techniques for different number of users with imperfect CSI.

Case 3. SE for different number of users and number of antennas with imperfect CSI

Case 4. SE performance analysis using linear precoding techniques at different BS number of antennas with perfect CSI.

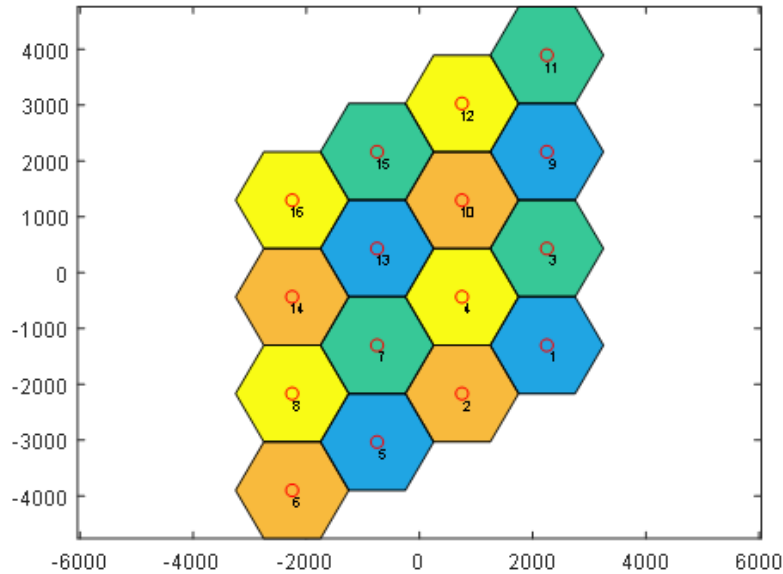
Case 5. SE performance evaluation using linear precoding techniques for different BS number of antennas and number of users having perfect CSI.

The parameters and their values for matlab simulation are listed under Table 4.1.

Figure 4.1, 4.2 and 4.3 illustrate 16-cell cluster with pilot reuse $N=4$, 12-cell cluster with pilot reuse $N=3$ and 16-cell cluster with pilot reuse $N=1$ respectively. Each pattern is associated with a different set of orthogonal pilots. These are also mutually orthogonal from pilot reuse pattern to pattern. In Figure 4.1, 4.2 the cells are described that the n^{th} cell and the $(n \pm N)^{\text{th}}$ cell use the same set of orthogonal pilots. In other word, the cells that have the same color use the same set of orthogonal pilots while the cells that have different color use different set of orthogonal pilots. Consequently, inter-cell interference or PC is reduced within cells. Each cell has different color with its neighboring cells. For example, the neighboring cells for cell 4 with pilot reuse $N=4$ are cell 1, 2, 3,7,10 and 13 that have distinct color with cell 4. Figure 4.3 shows all cells have the same color this

Table 4.1: parameters and values

parameters	values (considerations)
Number of cells	Multi-cells (16 [29], 12)
Cell radius	1000m [26]
Channel state information	Perfect and imperfect CSI at the BS
Channel model	Correlated Rayleigh fading
Number of antennas per BS (Fixed)	100 [28]
Range of antennas per BS (When varied)	10-110
Number of users (Fixed)	10 [28]
Number of users(Varied)	0-40 [25]
UL and DL power	20dBm [29]
PRF	1,3,4
Channel gain at 1 km (Υ)	148.1 dB [29]
Path-loss exponent (α)	3.76 [29]
Receiver noise power	94 dBm [29]
Bandwidth	20MHz [3]
Carrier frequency	2GHz [3]
Coherence interval	300 [3]
Number of channel realizations	100
Shadow fading standard deviation (σ_{sf})	10dB [29]

**Figure 4.1:** 16-cell cluster with pilot reuse $N=4$.

indicates that all the k^{th} user use the same pilot.

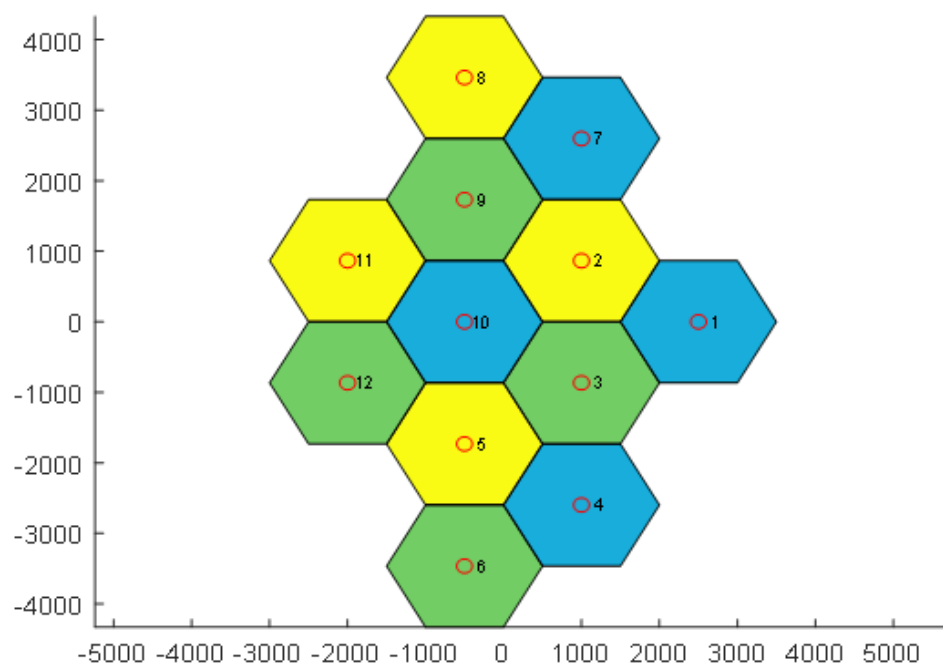


Figure 4.2: 12-cell cluster with pilot reuse $N=3$

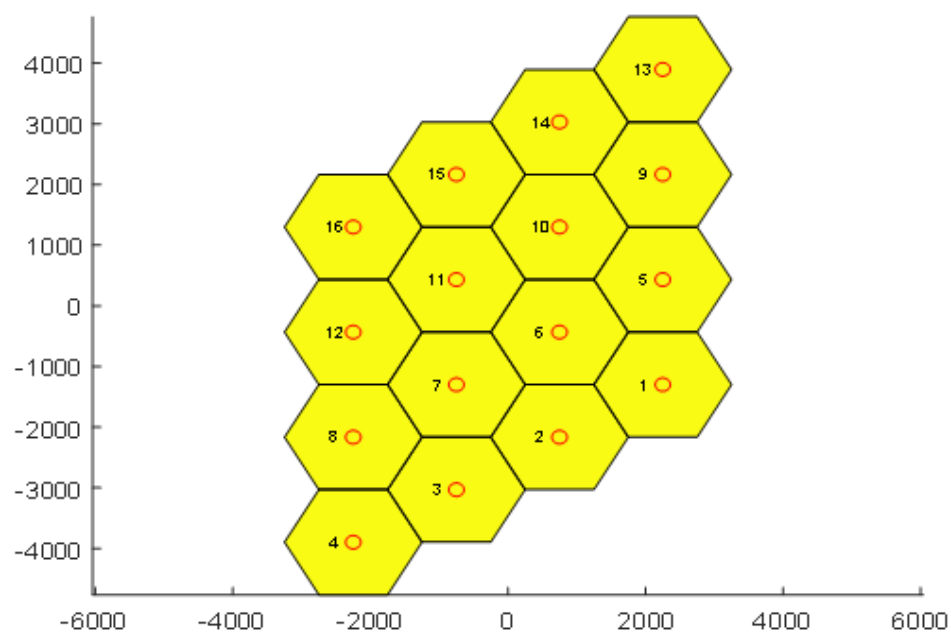


Figure 4.3: 16-cell cluster with pilot reuse $N=1$

4.2 Spectral Efficiency for different number of BS antennas with imperfect CSI

We assume the number of users per cell, $K = 10$ [25] and vary the number of BS antennas from 10 to 110. We consider a communication bandwidth of 20MHz, an UL transmit power of 20dBm per user and each BS allocates 20dBm DL transmit power (assume the power is same for each user). The pilot signal length is $\tau_p = NK$, where the integer, N is the pilot reuse factor (specifically $N=1, 3, 4$). Thus, the number of pilots are increased by N - times than users for each cell. These pilots are randomly assigned to the users in each cell. Rayleigh fading channel under local scattering spatial channel correlation model with given nominal arrival angle, 30° and Gaussian angular standard deviation, $\sigma_\varphi = 10^\circ$ are considered for SE evaluation of Ma-MIMO system.

Figure 4.4 shows the average sum SE versus number of BS antennas (M) for the three

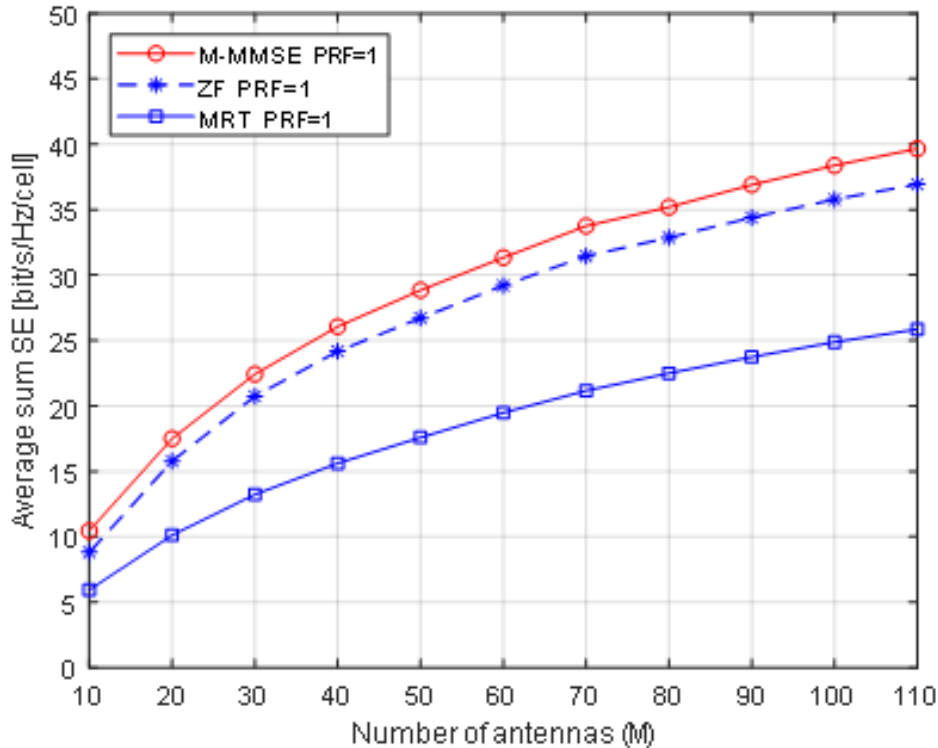


Figure 4.4: Average sum SE with respect to the number of BS antennas for M-MMSE, ZF and MRT precoding techniques (for a PRF of one and $K=10$)

precoding techniques and PRF of one. As we can see from the result the M-MMSE

provides the best performance than ZF and MRT precoding. The pilot reuse factor is one; the length of required pilot sequence τ_p is the same as number of users. Thus each cell reuses the same k pilots. Because M-MMSE can reduce the inter cell interference in addition to intra cell interference.

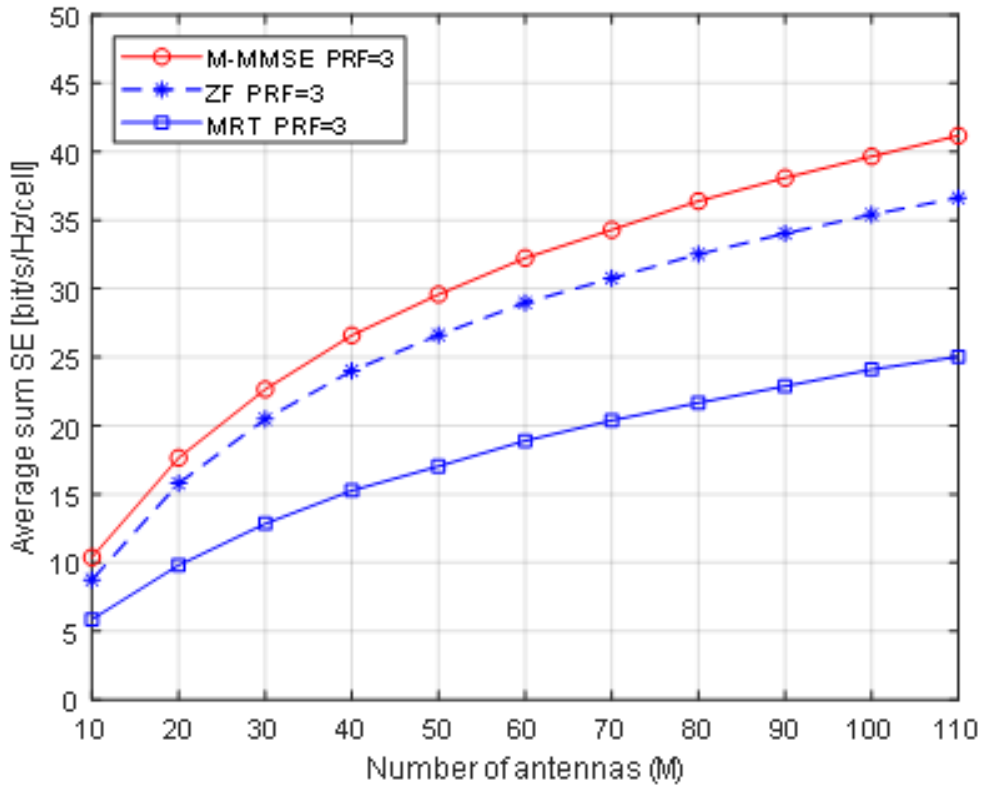


Figure 4.5: Average sum SE with respect to the number of BS antennas for M-MMSE, ZF and MRT precoding techniques (for a PRF of three and $K=10$)

Similarly, Figure 4.5 illustrates the SE of Ma MIMO with respect to the number of BS antennas for 3 reuse factor and the three precoding techniques. The figure shows that M-MMSE provides the best system performance. ZF shows better performance than MRT Precoding and MRT gives the lowest SE. The result also shows that average sum SE of M-MMSE Precoding with PRF of three are higher than this Precoding with PRF of one due to it can better suppress the interference from user terminals in the neighboring cells when these user terminals use other pilots. For 3 reuse factor the SE of MRT slightly reduces since the improved estimation quality does not outweigh the reduced pre-log factor when the estimate is only used to coherently combine the desired signal and not to cancel interference. likewise, the SE of ZF reduces for 3 reuse factor. Thus, ZF and MRT provide lower average sum SE.

Figure 4.6: shows that average sum SE increases as increase number of antennas and the PRF (i.e $N=4$) for M-MMSE Precoding. The cells are grouped into four pilot groups.

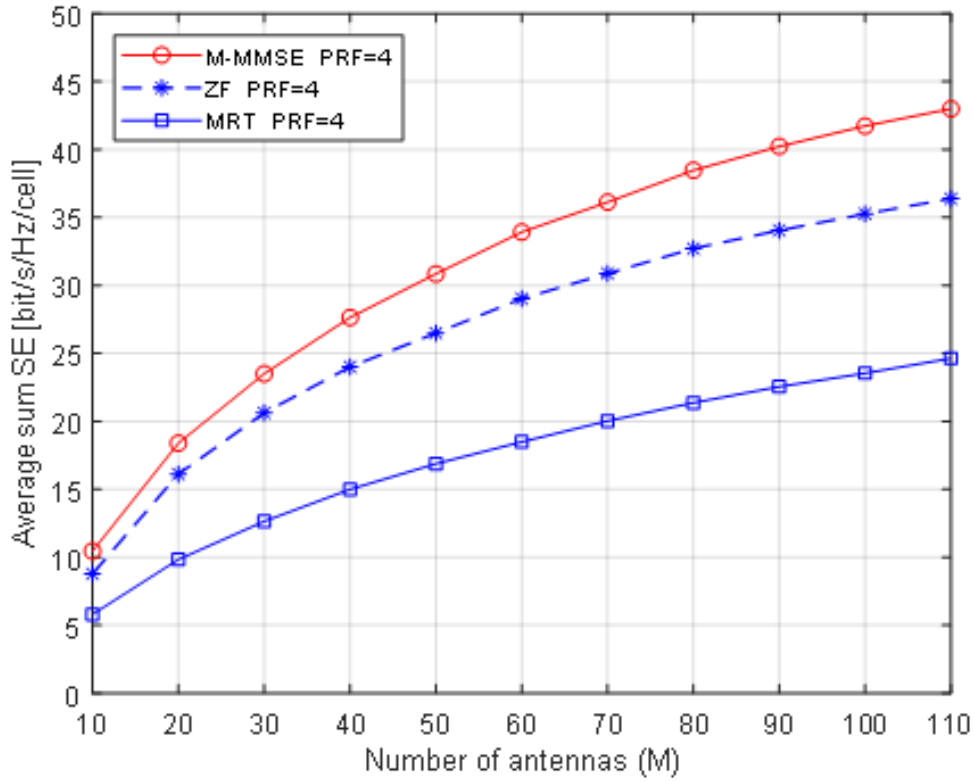


Figure 4.6: Average sum SE with respect to the number of BS antennas for MMSE, ZF and MRT precoding techniques a PRF of four and $K=10$

The cells in each group uses different orthogonal pilots. According to the pilot reuse pattern, the pilots are reused in different pilot group as result the PC is reduced and SE is increased.

Figure 4.4, 4.5 and 4.6 show average sum SE with respect to the number of BS antennas for MMSE, ZF and MRT with one, three and four PRF respectively. M-MMSE Precoder achieves higher SE than ZF and MRT for all taken PRFs and it has highest SE at PRFs of four among all because it reduces the level of PC by using different pilot for user terminals in surrounding cells and. MRT achieves the lowest SE performance for four reuse factor and it provides highest SE for one reuse factor. ZF achieves better performance than MRT Precoding.

4.3 Spectral Efficiency versus different number of users with imperfect CSI

Figure 4.7 shows average sum SE increases versus number of users for the three precoding techniques with PRF =1. As it can be seen MR (i.e. MRT) gives the lowest SE than all because MRT only increases the signal gain but it doesn't suppress the interference. and M-MMSE provides the best performance. The PRF is one; the number of users is the same as pilot sequence length, τ_p . The sum SE increases as number of user increases until its SE reaches saturation point. (Hint: MR in Figure 4.7, 4.8 and 4.9 is represent MRT precoding).

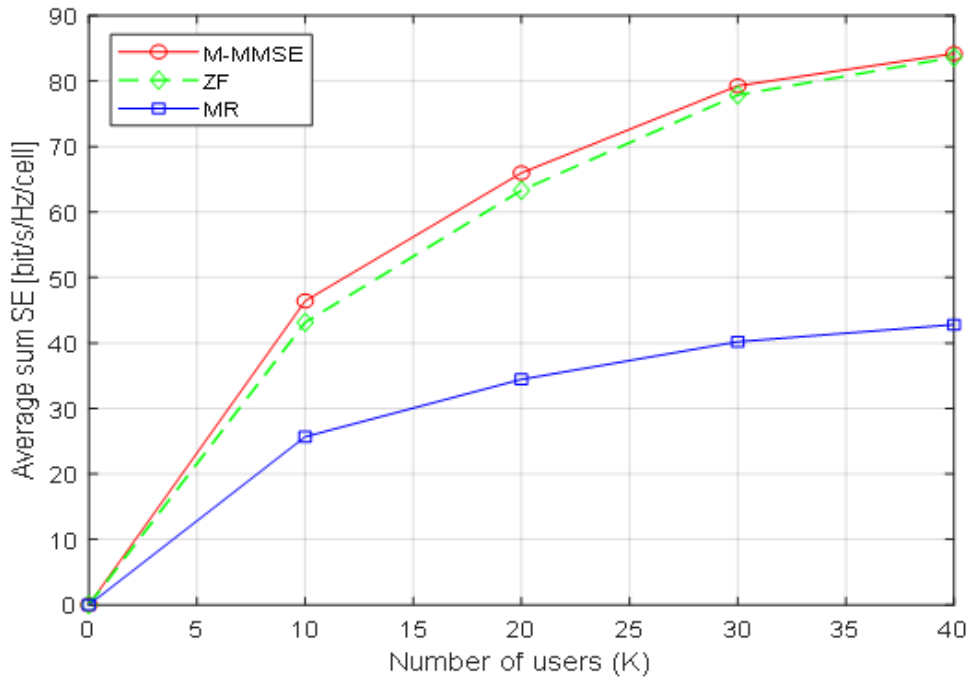


Figure 4.7: Average sum SE with respect to the number of users for M-MMSE, ZF and MRT precoding techniques (a PRF of one and M=100)

To look at the SE of the system for larger PRF, Figure 4.8 and Figure 4.9 are simulated for PRF 3 and 4 respectively. Figure 4.8 illustrates average sum SE versus of users' increases from 0 to 30 for all linear precoding techniques with PRF is three. The SE increases as number of users increase then reaches maximum point(at K=30) and finally decreases as number of users' increases from 30 to 40. Similar to figure 4.7, MRT gives the lowest SE and M-MMSE provides the best performance. ZF shows better performance than MR

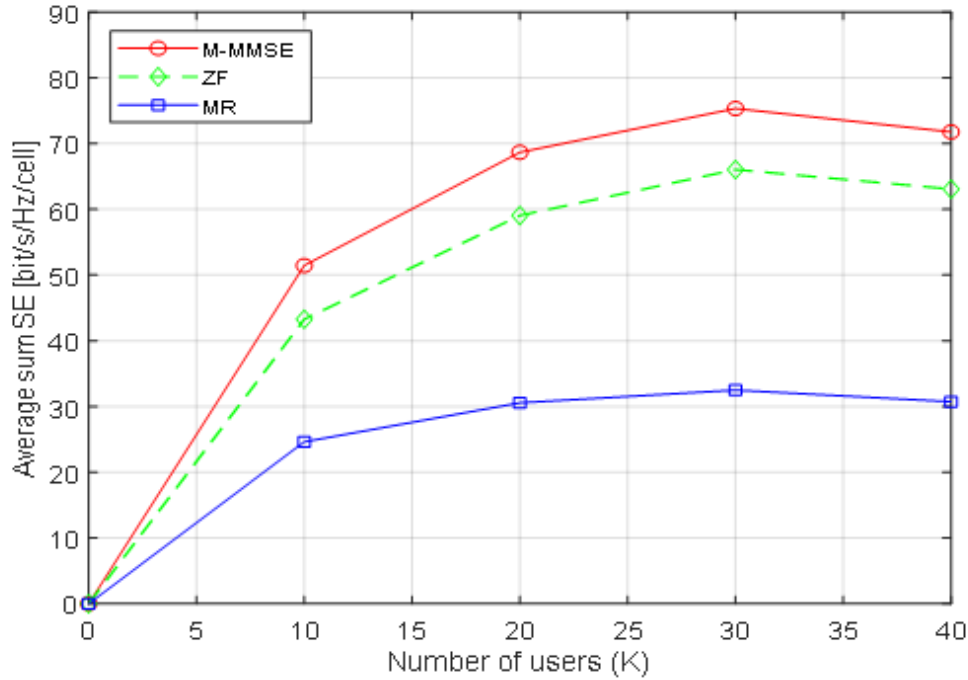


Figure 4.8: Average sum SE with respect to the number of users for M-MMSE, ZF and MRT. Precoding techniques (for a PRF of three and $M=100$)

Precoding. The PRF is three; the required pilot sequence length is three times of number of users.

Figure 4.9 shows, first average sum SE increases as number of users increases for all linear precoding techniques with PRF is four, then reaches maximum point and keeps constant (from $K=20$ to 30 for M-MMSE and MRT) and finally decreases as number of users' increases from 30 to 40. The result shows that MRT and ZF provides lower performance than M-MMSE. MRT gives the lowest SE. The pilot group is divided into four and the length of pilot sequence is four times of K .

Average sum SE decreases as number of users' increases from 0 to 40 for all linear precoding techniques with PRF changes from one to three and four as shown Figure 4.9 because PRF 3 and 4 are effective at small number of users. The SE of three precodings reaches saturation level (maximum point) for different number of users due to the precodings performance depends the coherence block.

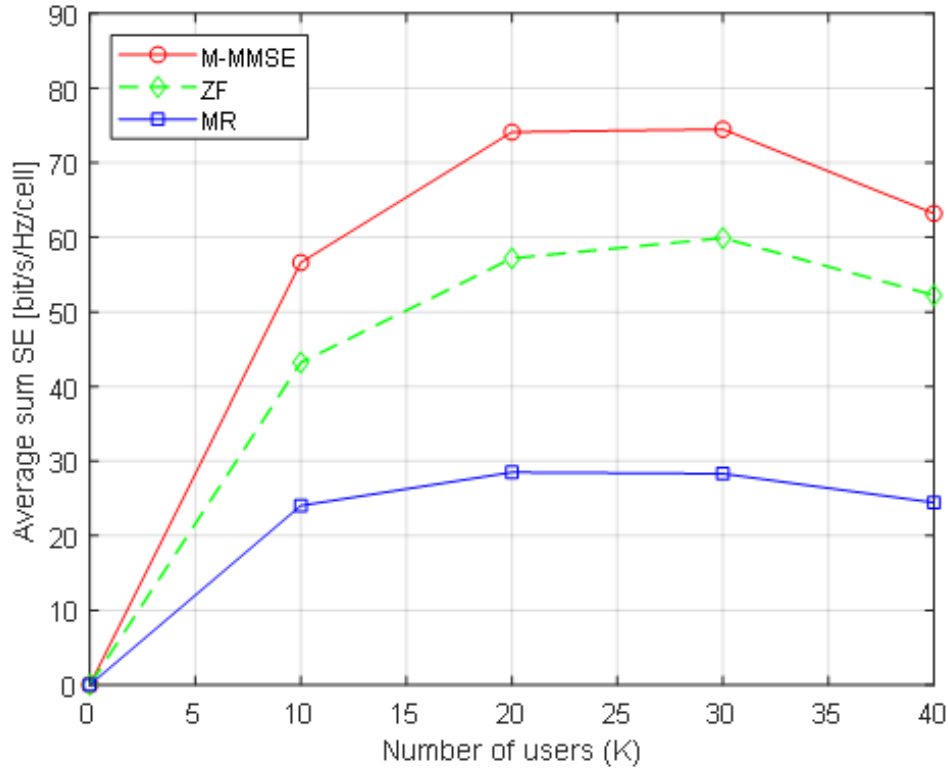


Figure 4.9: Average sum SE with respect to the number of users for MMSE, ZF and MRT precoding techniques and a PRF of four ($M=100$)

4.4 Spectral Efficiency for different number of users and number of antennas with imperfect CSI

We used the number of users per cell, $K = 10$ and $K=20$, change the number of antennas from 10 to 110 per BS and keeping the PRF is fixed, that is $N=4$.

Figure 4.10 shows that the SE increases as the number of antennas at the BS increases and the same PRF is used and number of users per cell is 10.

Table 4.2: SE values at specified values of BS antennas in the range $M=10$ to 110 and number of users per cell ($K=10$)

Precoding techniques combined with PRF	SE				
	M=10	M=30	M=50	M=80	M=100
MRT PRF=4	6	13	17	22	25
ZF PRF=4	9	21	26.53	33	36
M-MMSE PRF=4	11	23	20.55	38.55	43

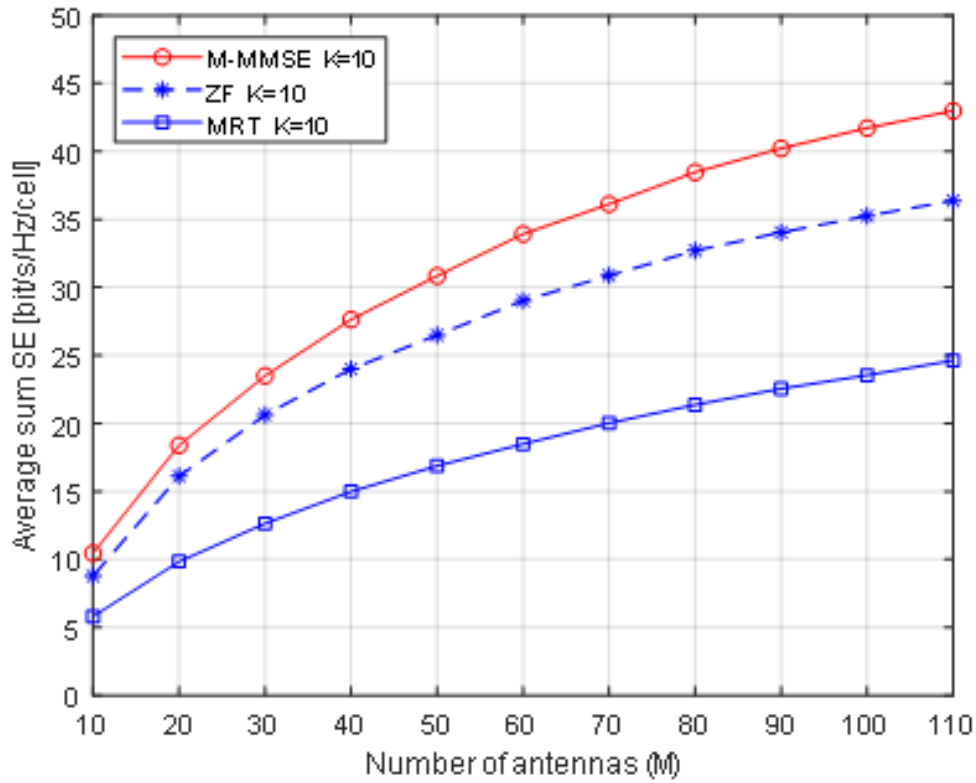


Figure 4.10: Average sum SE with respect to the number of antennas for M-MMSE, ZF and MRT precoding techniques (for a PRF=4 and K=10)

Figure 4.11 shows that the SE increases as the number of BS antennas increases and users per cell is increased from 10 to 20 and also the same PRF is used. The result also shows that the sum SE is better when the number of users per cell is changed from k=10 to 20 and the number of BS antennas is also changed.

Table 4.3: SE numerical values at specified values of BS antennas in the range M=10 to 110 and number of users per cell (K=20)

Precoding techniques combined with PRF	SE				
	M=10	M=30	M=50	M=80	M=100
MRT PRF=4	5.6	13.62	19.18	25.31	28.56
ZF PRF=4	8.63	23.8	35.42	46	50.6
M-MMSE PRF=4	9.8	28.59	45.7	53.5	59.9

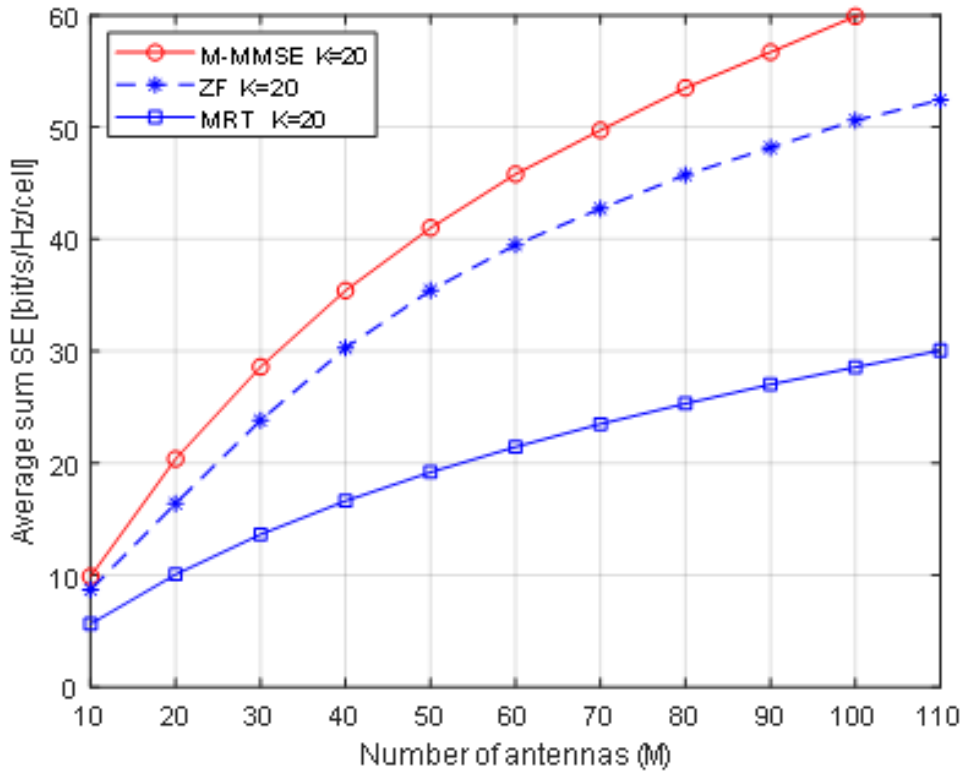


Figure 4.11: Average sum SE with respect to the number of antennas for MMSE, ZF and MRT precoding techniques (for a PRF=4 and K=20)

4.5 Spectral Efficiency for different number of BS antennas with perfect CSI

We used the number of users per cell, $K = 10$ and change the number of BS antennas from 10 to 110. We consider a communication bandwidth of 20MHz, an UL transmit power of 20dBm per user and each BS allocates 20dBm DL transmit power. Figure 4.12 depicts the average sum SE versus number of antennas (M) for the three precoding techniques. As Figure 4.12 shows the SE increases as the number of antennas increase for all linear precoding techniques. MMSE and ZF provide higher SE than MRT precoding and have almost the same performance a

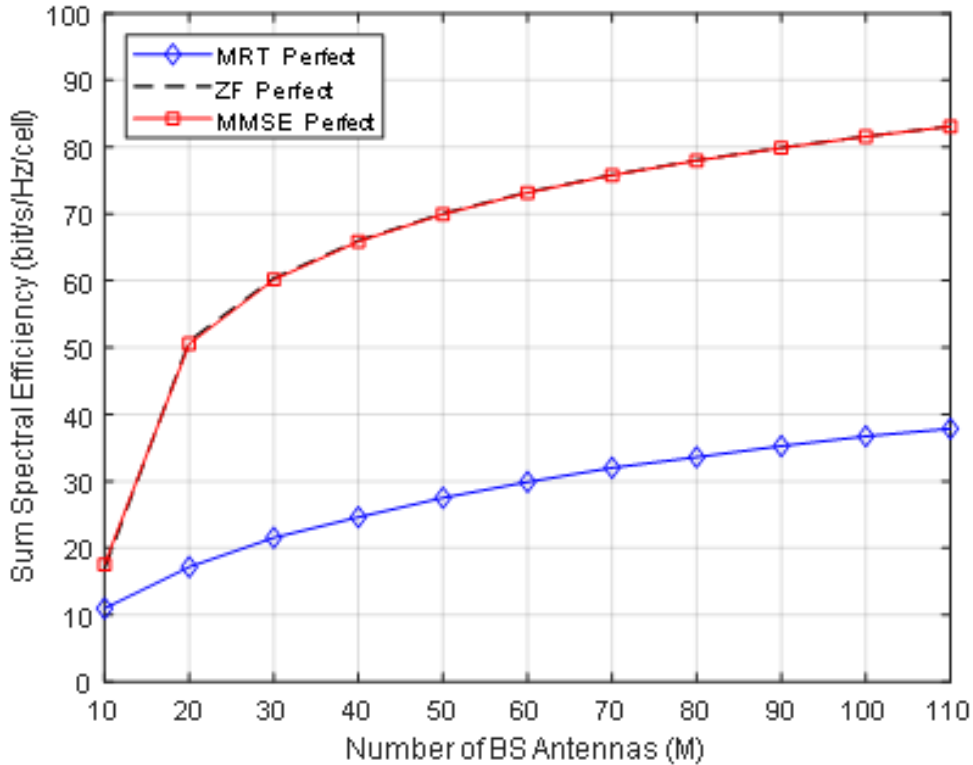


Figure 4.12: Average sum SE with respect to the number of BS antennas for MMSE, ZF and MRT precoding techniques (for $K=10$ and $SNR=5dB$)

4.6 Spectral Efficiency for both different number of users and BS antennas with perfect CSI

We used the number of antennas from 10 to 110 per BS and the number of users per cell, $K = 10$ and $K=20$ change (i.e. when both K and M are changed simultaneously). We consider a communication bandwidth of 20MHz, an UL transmit power of 20dBm per user and each BS allocates 20dBm DL transmit power.

Figure 4.13 shows that the average sum SE increases linearly as the number of antennas and users increase for all linear precoding techniques. MMSE and ZF provide higher SE. ZF achieves better performance than MRT, but almost the same as MMSE, and MRT achieves lowest performance for all considered number of BS antennas. The result also shows that the sum SE increases as the number of users and Antennas are increase at the same time and $M \gg K$ (M/K increases) because it becomes easier to suppress interference.

Figure 4.14 shows that the SE increases slowly with small number of BS antennas and the

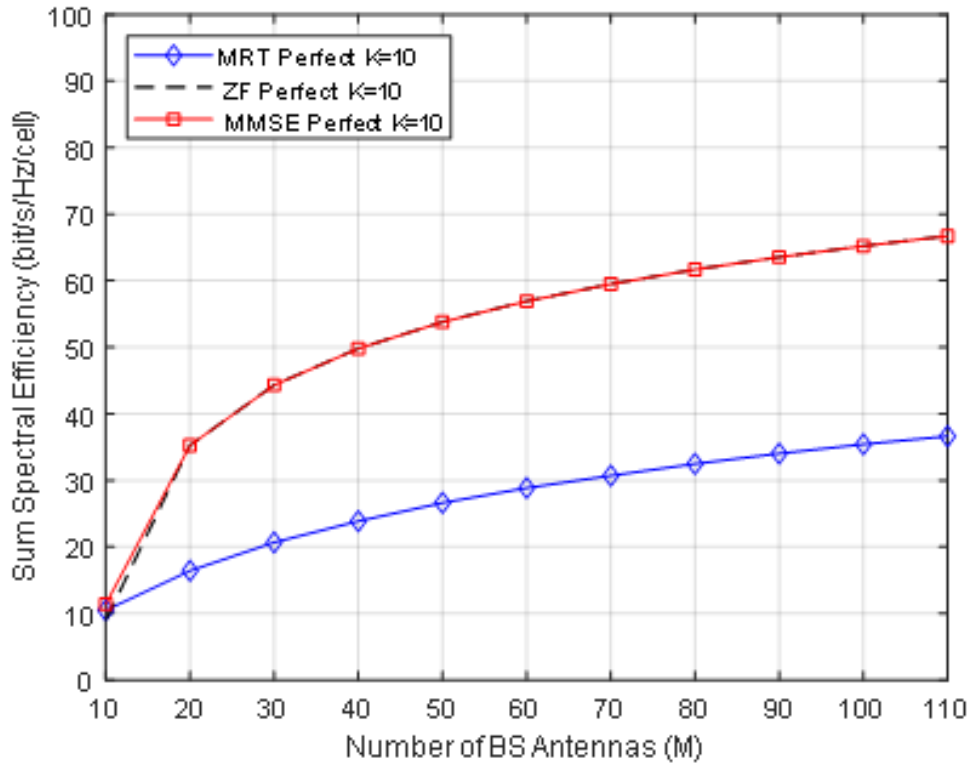


Figure 4.13: Average sum SE with respect to the number of antennas for MMSE, ZF and MRT precoding techniques (for $K=10$ and $SNR=0dB$)

Table 4.4: SE numerical values at specified values of BS antennas in the range $M=10$ to 110 and number of users per cell ($K=10$)

Precoding techniques	SE				
	M=10	M=30	M=50	M=80	M=110
MRT	10	20	28	29.85	36.75
ZF	10	45	53.55	60	67
MMSE	10	45	53.55	60	67

number of users is changed from 10 to 20. This is because the BS does not have enough spatial degrees of freedom to separate the users. For example, at $K=20$ and M less than 20, but at $K=20$ and M greater than 20 the spectral efficiency increases effectively due to the BS has enough spatial degrees of freedom to separate the users. The result also shows that the sum SE is better when the users per cell is changed from $k=10$ to 20 and the number of BS antennas is also changed.

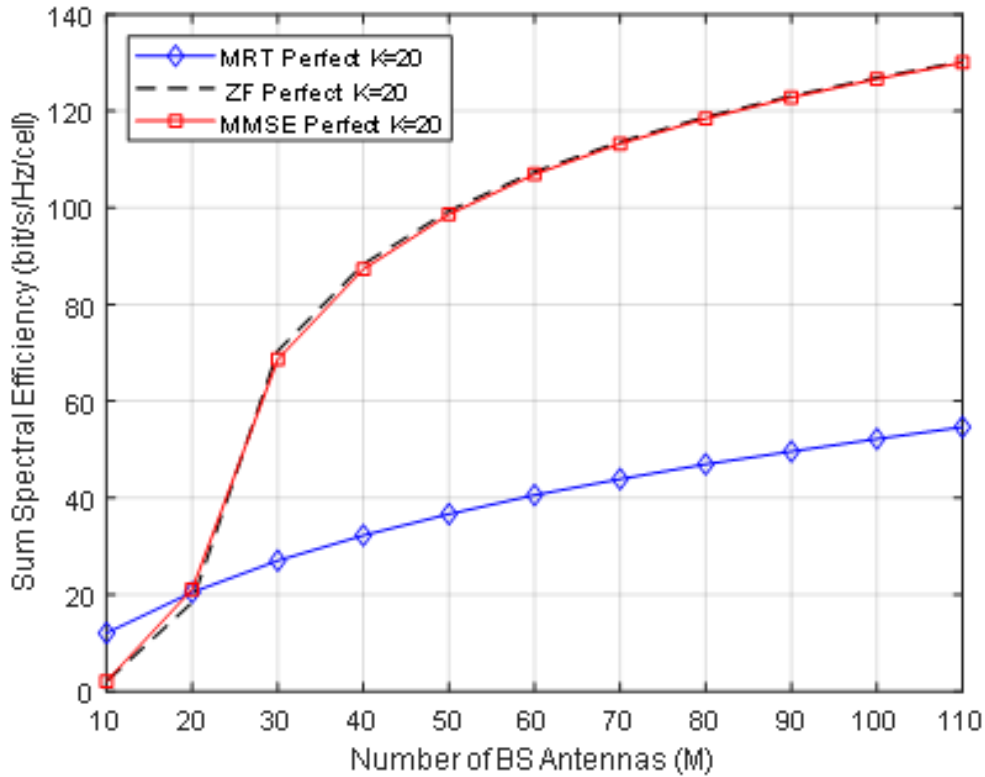


Figure 4.14: Average sum SE with respect to the number of antennas for MMSE, ZF and MRT precoding techniques (for $K=20$ and $SNR=0dB$)

Table 4.5: SE numerical values at specified values of BS antennas in the range $M=10$ to 110 and number of users per cell ($K=20$)

Precoding techniques	SE				
	M=10	M=30	M=50	M=80	M=110
MRT	10	24	38	44	57
ZF	1.25	65	100	119.25	125
MMSE	1.25	55	100	119.25	125

When we compare the SE of the system using all linear precoding techniques (MRT, ZF and MMSE) with both imperfect and perfect CSI, the SE of the system using linear precoding techniques with perfect CSI achieve better performance than their corresponding precoding techniques under imperfect CSI during changing the number of BS antennas from 10 to 110 and fixed number of users, $K=10$.

/

Conclusion and Future Works

5.1 Conclusion

A Ma-MIMO system gives higher SE without increasing frequency spectrum. This system uses linear precoding techniques like MRT, ZF, MMSE and M-MMSE at the BS. The known channel is estimated from the UL via TDD mode and MMSE estimation is used. The SINR and SE are derived for both perfect and imperfect CSI.

In this thesis, we have analyzed and evaluated the performance of multicell DL Ma-MIMO system using linear precoding techniques and PRF under spatially correlated Rayleigh fading channel model with both perfect CSI and Imperfect CSI for different BS number of antennas and number of users per cell. M-MMSE Precoder achieves higher SE than ZF and MRT for all taken pilot reuse factors due to it can better suppress the inter cell interference of users in neighboring cells for using fixed number of users and for different BS number of antennas when these user terminals use other pilots and also it has highest average sum SE at PRF of four among all because it reduces the level of PC. ZF achieves better performance than MRT Precoding. The result also depicts that the sum SE is increased initially, then reach at optimal value and decreased finally when the number of users per cell is changed and fixed number of antennas is used even the PRF is increased. This indicates that large PRF is effective at small number of users and small pilot reuse factor is effective at large number of users. The sum SE is increased when both the number of users (K) and antennas (M) are changed at the same time. The sum SE of all precoder with perfect CSIT better than the sum SE of all precoder with imperfect CSIT. It exceeds the sum SE of all precoder with imperfect CSIT by more than 25% for $M \gg K$.

5.2 Recommendations for Future Work

In this work, we investigated the SE performance of multicell Ma-MIMO system using PRF and precoding techniques. Even though performance evaluation is done by assuming different scenarios and assumptions, there are still cases and considerations that should need future investigation. Here we describe some the future works.

- In our thesis, we made performance evaluation by assuming the number of Antennas at user side is one (i.e. single antenna users) and limited by SE metrics.. But further investigation can be done by assuming multi antenna users.
- Performance evaluation can be also analyzed in-terms of EE and complexity metrics.
- We assumed Equal transmit power allocation in this thesis, It can be extended to Mu-cell Ma-MIMO Systems for optimization strategy using power allocation algorithms.

Bibliography

- [1] Ezio Biglieri, Robert Calderbank, Anthony Constantinides, Andrea Goldsmith, Arogyaswami Paulraj, and H Vincent Poor. *MIMO wireless communications*. Cambridge university press, 2007.
- [2] Fredrik Rusek, Daniel Persson, Buon Kiong Lau, Erik G Larsson, Thomas L Marzetta, Ove Edfors, and Fredrik Tufvesson. Scaling up mimo: Opportunities and challenges with very large arrays. *IEEE signal processing magazine*, 30(1):40–60, 2012.
- [3] Thomas L Marzetta and Hien Quoc Ngo. *Fundamentals of massive MIMO*. Cambridge University Press, 2016.
- [4] De Mi. *Massive MIMO with imperfect channel state information and practical limitations*. University of Surrey (United Kingdom), 2017.
- [5] Xiang Gao, Ove Edfors, Fredrik Rusek, and Fredrik Tufvesson. Massive mimo in real propagation environments. *IEEE Trans. Wireless Commun*, 2014.
- [6] Chi Feng. Interference analysis of massive mimo downlink with mrt precoding and applications in performance analysis. 2016.
- [7] Thomas L Marzetta. Massive mimo: an introduction. *Bell Labs Technical Journal*, 20:11–22, 2015.
- [8] Mariam Kawambwa. Pilot contamination mitigation techniques in massive mimo systems: A precoding approach. 2016.
- [9] Taesang Yoo and Andrea Goldsmith. On the optimality of multiantenna broadcast scheduling using zero-forcing beamforming. *IEEE Journal on selected areas in communications*, 24(3):528–541, 2006.
- [10] Quentin H Spencer, Christian B Peel, A Lee Swindlehurst, and Martin Haardt. An introduction to the multi-user mimo downlink. *IEEE communications Magazine*, 42(10):60–67, 2004.

-
- [11] Emil Björnson, Erik G Larsson, and Thomas L Marzetta. Massive mimo: Ten myths and one critical question. *IEEE Communications Magazine*, 54(2):114–123, 2016.
- [12] Thomas L Marzetta. Noncooperative cellular wireless with unlimited numbers of base station antennas. *IEEE transactions on wireless communications*, 9(11):3590–3600, 2010.
- [13] Olakunle Elijah, Chee Yen Leow, Tharek Abdul Rahman, Solomon Nunoo, and Solomon Zakwoi Iliya. A comprehensive survey of pilot contamination in massive mimo—5g system. *IEEE Communications Surveys & Tutorials*, 18(2):905–923, 2015.
- [14] Weiqiang Tan, Wei Huang, Xi Yang, Zheng Shi, Wen Liu, and Lisheng Fan. Multiuser precoding scheme and achievable rate analysis for massive mimo system. *EURASIP Journal on Wireless Communications and Networking*, 2018(1):1–12, 2018.
- [15] Hien Quoc Ngo. *Massive MIMO: Fundamentals and system designs*, volume 1642. Linköping University Electronic Press, 2015.
- [16] Kemal Davaslioglu and Richard D Gitlin. 5g green networking: Enabling technologies, potentials, and challenges. In *2016 IEEE 17th Annual Wireless and Microwave Technology Conference (WAMICON)*, pages 1–6. IEEE, 2016.
- [17] Erik G Larsson, Ove Edfors, Fredrik Tufvesson, and Thomas L Marzetta. Massive mimo for next generation wireless systems. *IEEE communications magazine*, 52(2):186–195, 2014.
- [18] Hien Quoc Ngo, Erik G Larsson, and Thomas L Marzetta. Aspects of favorable propagation in massive mimo. In *2014 22nd European Signal Processing Conference (EUSIPCO)*, pages 76–80. IEEE, 2014.
- [19] Ananthanarayanan Chockalingam and B Sundar Rajan. *Large MIMO systems*. Cambridge University Press, 2014.
- [20] Lu Lu, Geoffrey Ye Li, A Lee Swindlehurst, Alexei Ashikhmin, and Rui Zhang. An overview of massive mimo: Benefits and challenges. *IEEE journal of selected topics in signal processing*, 8(5):742–758, 2014.

-
- [21] Jakob Hoydis, Stephan Ten Brink, and Mérouane Debbah. Massive mimo in the ul/dl of cellular networks: How many antennas do we need? *IEEE Journal on selected Areas in Communications*, 31(2):160–171, 2013.
- [22] Xudong Zhu, Zhaocheng Wang, Linglong Dai, and Chen Qian. Smart pilot assignment for massive mimo. *IEEE Communications Letters*, 19(9):1644–1647, 2015.
- [23] Mei Zhao, Haixia Zhang, Shuaishuai Guo, and Dongfeng Yuan. Joint pilot assignment and pilot contamination precoding design for massive mimo systems. In *2017 26th Wireless and Optical Communication Conference (WOCC)*, pages 1–6. IEEE, 2017.
- [24] Pengbiao Wang, Chenglin Zhao, Yongjun Zhang, Yang Zhang, and Gordon L Stuber. A novel pilot assignment approach for pilot decontaminating in massive mimo systems. In *2017 IEEE Wireless Communications and Networking Conference (WCNC)*, pages 1–6. IEEE, 2017.
- [25] Abhishek Thakur and Ramesh Chandra Mishra. Performance analysis of energy-efficient multi-cell massive mimo system. In *2019 10th International Conference on Computing, Communication and Networking Technologies (ICCCNT)*, pages 1–7. IEEE, 2019.
- [26] Muhammad Hassan, Muhammad Zia, Awais Ahmed, and Naeem Bhatti. Pilot contamination attack detection for multi-cell mu-massive mimo system. *AEU-International Journal of Electronics and Communications*, 113:152945, 2020.
- [27] Saba Qasim Jabbar and Yu Li. Analysis and evaluation of performance gains and tradeoffs for massive mimo systems. *Applied Sciences*, 6(10):268, 2016.
- [28] Adeeb Salh, Lukman Audah, Nor Shahida Mohd Shah, and Shipun Anuar Hamzah. Mitigating pilot contamination for channel estimation in multi-cell massive mimo systems. *Wireless Personal Communications*, 112(3):1643–1658, 2020.
- [29] Emil Björnson, Jakob Hoydis, and Luca Sanguinetti. Massive mimo networks: Spectral, energy, and hardware efficiency. *Foundations and Trends in Signal Processing*, 11(3-4):154–655, 2017.

-
- [30] Cheng-Xiang Wang, Ji Bian, Jian Sun, Wensheng Zhang, and Minggao Zhang. A survey of 5g channel measurements and models. *IEEE Communications Surveys & Tutorials*, 20(4):3142–3168, 2018.
- [31] Ferdous Hossain, Tan Kim Geok, Tharek Abd Rahman, Mohammad Nour Hindia, Kaharudin Dimiyati, Sharif Ahmed, Chih P Tso, and Noor Ziela Abd Rahman. An efficient 3-d ray tracing method: Prediction of indoor radio propagation at 28 ghz in 5g network. *Electronics*, 8(3):286, 2019.
- [32] Hao Jiang and Guan Gui. *Channel Modeling in 5G Wireless Communication Systems*. Springer, 2020.
- [33] Theodore S Rappaport et al. *Wireless communications: principles and practice*, volume 2. prentice hall PTR New Jersey, 1996.
- [34] Gamini Senarath. Multi-hop relay system evaluation methodology (channel model and performance metric). http://iee802.org/16/relay/docs/80216j-06_013r3.pdf, 2007.
- [35] Muhammad RA Khandaker and Kai-Kit Wong. Signal processing for massive mimo communications. In *Academic Press Library in Signal Processing, Volume 7*, pages 367–401. Elsevier, 2018.
- [36] Emil Björnson, Mats Bengtsson, and Björn Ottersten. Optimal multiuser transmit beamforming: A difficult problem with a simple solution structure [lecture notes]. *IEEE Signal Processing Magazine*, 31(4):142–148, 2014.